Alkyne Insertion into *cis*-Silyl(stannyl)platinum(II) Complexes

Takashi Sagawa, Yasunobu Sakamoto, Rika Tanaka, Hiroyuki Katayama,† and Fumiyuki Ozawa*,†

Department of Applied Chemistry, Graduate School of Engineering, Osaka City University, Sumiyoshi-ku, Osaka 558-8585, Japan

Received July 25, 2003

A series of *cis*-silyl(stannyl)platinum(II) complexes have been prepared by oxidative addition of silylstannanes to $Pt(cod)_2$ in toluene in the presence of tertiary phosphine ligands: *cis*-$Pt(SiR_3)(SnMe_3)L_2$ [L = PMe_2Ph, SiR_3 = $SiMe_3$ (**1a**), $SiMe_2Ph$ (**1b**), $SiMePh_2$ (**1c**), $SiPh_3$ (**1d**); SiR_3 = $SiMe_2Ph$, L = PMe_3 (**1e**), PEt_3 (**1f**), $PMePh_2$ (**1g**)]. These complexes undergo competitive insertion of alkynes (R′C≡CH) into the Pt−Sn and Pt−Si bonds under kinetic conditions to give the insertion complexes *cis*-$Pt\{C(R')=CHSnMe_3\}(SiR_3)L_2$ (**2**) and *cis*-$Pt(SnMe_3)\{C(R')=CHSiR_3\}L_2$ (**3**), respectively. Furthermore, once **2** is formed in the reaction systems, it is converted to **3** under thermodynamic conditions. The kinetic ratio of **2** to **3** is significantly affected by the silyl and phosphine ligands as well as the alkynes employed. Thus, in the insertion of phenylacetylene, the kinetic ratio changes depending on the silyl and phosphine ligands attached to the complexes as follows: **2**/**3** = 0/100 (**1a**), 30/70 (**1b**), 59/41 (**1c**), 93/7 (**1d**), 36/64 (**1e**), 25/75 (**1f**), 25/75 (**1g**). On the other hand, in the reactions of **1b**, the kinetic ratio varies with alkynes as follows: **2**/**3** = 12/88 (*p*-$H_2NC_6H_4C$≡CH), 28/72 (*p*-MeC_6H_4C≡CH), 30/70 (PhC≡CH), 46/54 (*p*-$OHCC_6H_4C$≡CH), 100/0 (MeO_2-CC≡CCO_2Me). Reasons for the variations are discussed on the basis of the insertion mechanism elucidated by kinetic investigations.

Introduction

Addition of inter-element linkages to carbon−carbon multiple bonds catalyzed by group 10 metal complexes has attracted a great deal of recent interest.[1] Scheme 1 shows a generally accepted catalytic cycle for the reaction using a terminal alkyne as a substrate, which consists of three elementary processes a−c. Oxidative addition of an element−element bond to a low-valent metal species (**A**) gives intermediate **B** bearing two metal−element bonds (process a), which subsequently undergoes insertion of alkyne into one of the metal−element bonds to give insertion complex **C** or **C′** (process b). Reductive elimination from **C** or **C′** forms addition product **D** with regeneration of **A** (process c). We are currently interested in the mechanisms of processes b and c,[2−4] which have been much less explored than the oxidative addition process a.[1]

Scheme 1

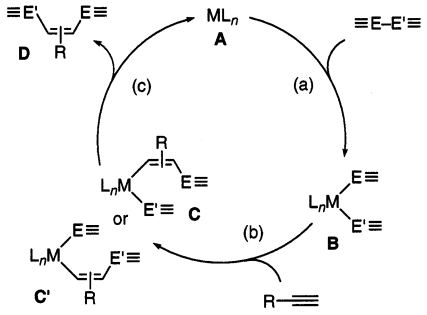

In this paper, we wish to describe a detailed mechanistic study of alkyne insertion into *cis*-silyl(stannyl)-platinum(II) complexes, which are models of key intermediates for palladium-catalyzed silylstannylation of unsaturated hydrocarbons.[5] Although this process has

* Corresponding author. E-mail: ozawa@scl.kyoto-u.ac.jp.
† Present address: Institute for Chemical Research, Kyoto University, Uji, Kyoto 611-0011, Japan.

(1) (a) Beletskaya, I.; Moberg, C. *Chem. Rev.* **1999**, *99*, 3435. (b) Han, L.-B.; Tanaka, M. *Chem. Commun.* **1999**, 395. (c) Suginome, M.; Ito, Y. *Chem. Rev.* **2000**, *100*, 3221. (d) Kondo, T.; Mistudo, T. *Chem. Rev.* **2000**, *100*, 3205.

(2) (a) Ozawa, F. *J. Organomet. Chem.* **2000**, *611*, 332. (b) Ozawa, F.; Kamite, J. *Organometallics* **1998**, *17*, 5630. (c) Sagawa, T.; Asano, Y.; Ozawa, F. *Organometallics* **2002**, *21*, 5879. (d) Ozawa, F.; Hikida, T. *Organometallics* **1996**, *15*, 4501. (e) Hikida, T.; Onitsuka, K.; Sonogashira, K.; Hayashi, T.; Ozawa, F. *Chem. Lett.* **1995**, 985. (f) Ozawa, F.; Sugawara, M.; Hayashi, T. *Organometallics* **1994**, *13*, 3237. (g) Ozawa, F.; Sugawara, M.; Hasebe, K.; Hayashi, T. *Inorg. Chim. Acta* **1999**, *296*, 19. (h) Hasebe, K.; Kamite, J.; Mori, T.; Katayama, H.; Ozawa, F. *Organometallics* **2000**, *19*, 2022. (i) Ozawa, F.; Kitaguchi, M.; Katayama, H. *Chem. Lett.* **1999**, 1289. (j) Ozawa, F.; Hikida, T.; Hasebe, K.; Mori, T. *Organometallics* **1998**, *17*, 1018. (k) Ozawa, F.; Hikida, T.; Hayashi, T. *J. Am. Chem. Soc.* **1994**, *116*, 2844. (l) Ozawa, F.; Mori, T. *Organometallics* **2003**, *22*, in press.

(3) For related mechanistic studies, see: (a) Iverson, C. N.; Smith, M. R., III. *Organometallics* **1996**, *15*, 5155. (b) Lesley, G.; Nguyen, P.; Taylor, N. J.; Marder, T. B. *Organometallics* **1996**, *15*, 5137. (c) Mochida, K.; Wada, T.; Suzuki, K.; Hatanaka, W.; Nishiyama, Y.; Nanjo, M.; Sekine, A.; Ohashi, Y.; Sakamoto, M.; Yamamoto, A. *Bull. Chem. Soc. Jpn.* **2001**, *74*, 123. (d) Ananikov, V.; Beletskaya, I.; Aleksandrov, G.; Eremenko, I. *Organometallics* **2003**, *22*, 1414.

(4) For theoretical treatment of catalytic processes, see: (a) Hada, M.; Tanaka, Y.; Ito, M.; Murakami, M.; Amii, H.; Ito, Y.; Nakatsuji, H. *J. Am. Chem. Soc.* **1994**, *116*, 8754. (b) Sakaki, S.; Ogawa, M.; Musashi, Y. *J. Organomet. Chem.* **1997**, *535*, 25. (c) Bottoni, A.; Higueruelo, A. P.; Miscione, G. P. *J. Am. Chem. Soc.* **2002**, *124*, 5506. (d) Cui, Q.; Musaev, D. G.; Morokuma, K. *Organometallics* **1997**, *16*, 1355. (e) Sakaki, S.; Kikuno, K. *Inorg. Chem.* **1997**, *36*, 226. (f) Cui, Q.; Musaev, D. G.; Morokuma, K. *Organometallics* **1998**, *17*, 1383.

10.1021/om030553t CCC: $25.00
Publication on Web 09/20/2003

Scheme 2

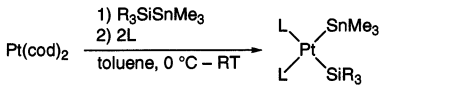

	SiR_3	L
1a	$SiMe_3$	PMe_2Ph
1b	$SiMe_2Ph$	PMe_2Ph
1c	$SiMePh_2$	PMe_2Ph
1d	$SiPh_3$	PMe_2Ph
1e	$SiMe_2Ph$	PMe_3
1f	$SiMe_2Ph$	PEt_3
1g	$SiMe_2Ph$	$PMePh_2$

been once examined theoretically,[4a] its experimental study has been extremely limited to date,[6] probably due to instability of silyl(stannyl)palladium(II) complexes. On the other hand, we have found in this study that a series of platinum analogues are successfully prepared by oxidative addition of silylstannanes to platinum(0) complexes and detailed information about the insertion mechanism is gained by kinetic examinations.[7] A particular interest has been focused on site selectivity in alkyne insertion. Thus, silyl(stannyl) complexes have two metal−element bonds capable of undergoing the insertion. A previous theoretical study using *cis*-Pd(SiH_3)(SnH_3)(PH_3)$_2$ has predicted that insertion into the Pd−Sn bond is preferable to that into the Pd−Si bond under kinetic conditions.[4a] On the other hand, for the platinum analogues, relative ease of the insertion into Pt−Si and Pt−Sn bonds has been found to dramatically vary with the types of silyl and phosphine ligands and alkynes employed.

Results

Synthesis of *cis*-Pt(SiR_3)($SnMe_3$)L_2. Silyl-stannyl complexes listed in Scheme 2 were prepared by the reactions of Pt(cod)$_2$ with silylstannanes and phosphines. For example, Pt(cod)$_2$ was dissolved in toluene and successively treated with $Ph_3SiSnMe_3$ (1 equiv) and PMe_2Ph (2 equiv) at 0 °C. $^{31}P\{^1H\}$ NMR analysis of the resulting solution revealed selective formation of **1d**, which was isolated as a yellow crystalline solid in 38% yield. In this procedure, $Ph_3SiSnMe_3$ must be added prior to PMe_2Ph; otherwise Pt(cod)(PMe_2Ph)$_2$ is exclusively formed in the system. Similar phenomena occurred for all silyl-stannyl complexes. Especially, PMe_3-coordinated **1e** was obtained as a 1:1 mixture with Pt(cod)(PMe_3)$_2$ even in the proper order of addition, while Pt(cod)(PMe_3)$_2$ was successfully removed by washing the crude product with Et_2O−pentane (1:3), and **1e** was isolated as an analytically pure compound in 35% yield.

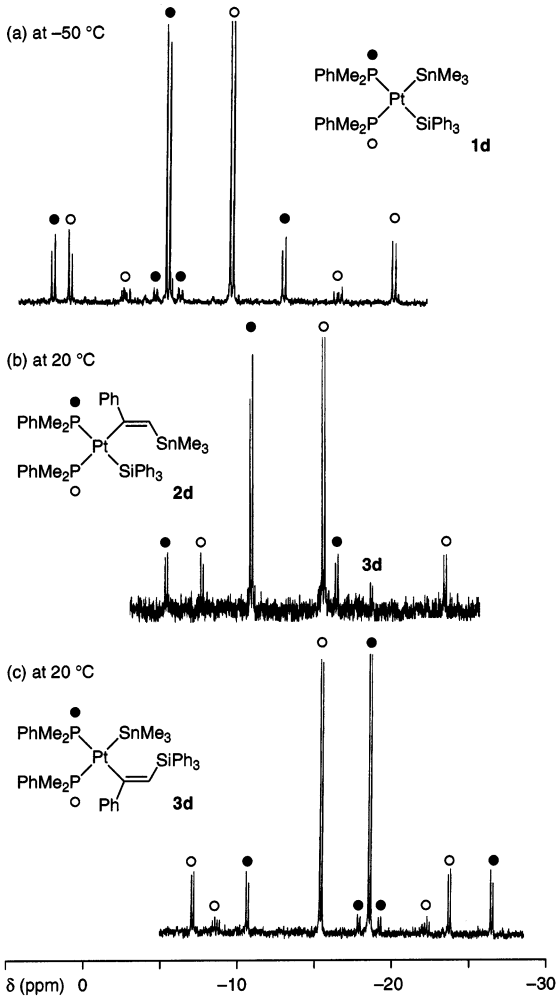

Figure 1. $^{31}P\{^1H\}$ NMR spectra of **1d**, **2d**, and **3d** in CD_2Cl_2 at 121.5 MHz. Complexes **1d** and **3d** were examined after isolation, whereas **2d** was generated in situ from **1d** and phenylacetylene (1.1 equiv) in CD_2Cl_2 in the presence of added PMe_2Ph (1 equiv) and examined without isolation. A broad singlet arising from free PMe_2Ph (δ −44.0) in spectrum b was omitted for simplicity.

Figure 1a shows the $^{31}P\{^1H\}$ NMR spectrum of **1d** measured at −50 °C in CD_2Cl_2. Two sets of doublets with ^{117}Sn, ^{119}Sn, and ^{195}Pt satellites are observed. The doublet at δ −9.7 with large $^2J_{SnP}$ couplings [1559 (^{119}Sn), 1499 Hz (^{117}Sn)] is due to the phosphine trans to the $SnMe_3$ ligand, whereas the other doublet at δ −5.4 with relatively small $^2J_{SnP}$ couplings [185 (^{119}Sn), 177 Hz (^{117}Sn)] is assignable to the phosphine cis to the $SnMe_3$ ligand (i.e., trans to the $SiPh_3$ ligand). The $^1J_{PtP}$ value for the latter signal (1663 Hz) is significantly smaller than that for the former one (2331 Hz), and this tendency is consistent with the greater trans influence of the silyl ligand than the stannyl ligand.

The $^{31}P\{^1H\}$ NMR signals of **1d** broadened at elevated temperature and coalesced into a broad singlet involving ^{195}Pt satellites at 35 °C (δ −7.6, $^1J_{PtP}$ = 1997 Hz). The coalescence temperature was not affected by addition of free PMe_2Ph (1 equiv) to the system. A similar type

(5) (a) Mitchell, T. N.; Killing, H.; Dicke, R.; Wickenkamp, R. *J. Chem. Soc., Chem. Commun.* **1985**, 354. (b) Chenard, B. L.; Laganis, E. D.; Davidson, F.; RajanBabu, T. V. *J. Org. Chem.* **1985**, *50*, 3666. (c) Chenard, B. L.; Van Zyl, C. M. *J. Org. Chem.* **1986**, *51*, 3561. (d) Mitchell, T. N.; Wickenkamp, R.; Amamria. A.; Dicke, R.; Schneider, U. *J. Org. Chem.* **1987**, *52*, 4868. (e) Murakami, M.; Amii, H.; Takizawa, N.; Ito, Y. *Organometallics* **1993**, *12*, 4223. (f) Obora, Y.; Tsuji, Y.; Asayama, M.; Kawamura, T. *Organometallics* **1993**, *12*, 4697. (g) Tsuji, Y.; Obora, Y. *J. Am. Chem. Soc.* **1991**, *113*, 9368. (h) Murakami, M.; Morita, Y.; Ito, Y. *J. Chem. Soc., Chem. Commun.* **1990**, 428. (i) Mitchell, T. N.; Schneider, U. *J. Organomet. Chem.* **1991**, *407*, 319. (j) Jeganmohan, M.; Shanmugasundaram, M.; Chang, K.-J.; Cheng, C.-H. *Chem. Commun.* **2002**, 2552. (k) Obora, Y.; Tsuji, Y.; Kakehi, T.; Kobayashi, M.; Shinkai, Y.; Ebihara, M.; Kawamura, T. *J. Chem. Soc., Perkin Trans. 1* **1995**, 599. (l) Mori, M.; Hirose, T.; Wakamatsu, H.; Imakuni, N.; Sato, Y. *Organometallics* **2001**, *20*, 1907. (m) Shin, S.; RajanBabu, T. V. *J. Am. Chem. Soc.* **2001**, *123*, 8416.

(6) Murakami, M.; Yoshida, T.; Kawanami, S.; Ito, Y. *J. Am. Chem. Soc.* **1995**, *117*, 6408.

(7) A part of this study has been communicated: Ozawa, F.; Sakamoto, Y.; Sagawa, T.; Tanaka, R.; Katayama, H. *Chem. Lett.* **1999**, 1307.

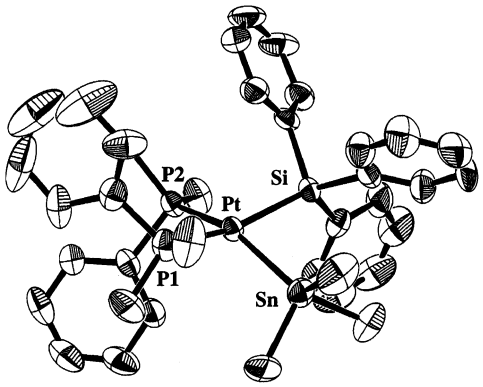

Figure 2. X-ray structure of **1d**·THF. Hydrogen atoms and THF molecule are omitted for clarity. Selected bond distances (Å) and angles (deg): Pt−Si = 2.362(2), Pt−Sn = 2.6079(5), Pt−P(1) = 2.352(2), Pt−P(2) = 2.323(2), Si−Pt−Sn = 86.20(5), P(1)−Pt-P(2) = 96.60(7), Si−Pt−P(1) = 158.76(7), Si−Pt−P(2) = 94.27(6), Sn−Pt−P(1) = 91.61-(5), Sn−Pt−P(2) = 154.69(5).

Scheme 3[a]

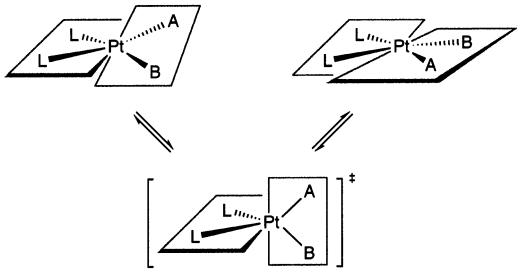

[a] A, B = SiR_3, $SnMe_3$.

of NMR behavior has already been documented for bis-(silyl)- and bis(stannyl)platinum(II) complexes by Tsuji et al. and attributed to the occurrence of twist-rotation via a pseudo-tetrahedral transition state on an NMR time scale (Scheme 3).[8] Although fluxional behavior of this type has never been observed for dialkylplatinum-(II) analogues, it becomes feasible when highly electron-releasing silyl and stannyl ligands are coordinated to platinum.

The structurally flexible nature of **1d** was also suggested by X-ray crystallography. As seen from the ORTEP diagram in Figure 2, the complex has significantly distorted square-planar geometry around platinum. The Pt−Si and Pt−Sn bonds are tilted from the PtP_2 plane by 18.2° and 24.0°, respectively, toward opposite directions from each other. Thus, the deviation from the ideal coordination plane is more remarkable for the $SnMe_3$ ligand than the $SiPh_3$ ligand, indicating more the flexible nature of the Pt−Sn bond than the Pt−Si bond. The Pt−P(1) bond (2.352(2) Å) trans to the silyl ligand is clearly longer than the Pt−P(2) bond (2.323(2) Å) trans to the stannyl ligand, reflecting the higher trans influence of the silyl ligand than the stannyl ligand.

Table 1 lists the $^{31}P\{^1H\}$ NMR data for **1a**−**g** at −50 °C, together with the coalescence temperatures for the two doublet signals. The signals due to the phosphines

Scheme 4

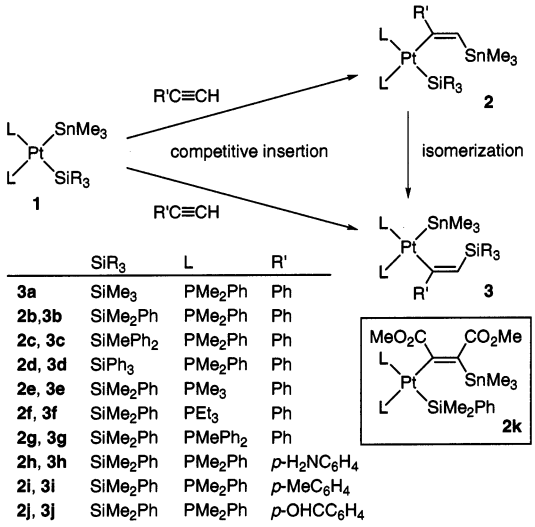

	SiR_3	L	R'
3a	$SiMe_3$	PMe_2Ph	Ph
2b,3b	$SiMe_2Ph$	PMe_2Ph	Ph
2c, 3c	$SiMePh_2$	PMe_2Ph	Ph
2d, 3d	$SiPh_3$	PMe_2Ph	Ph
2e, 3e	$SiMe_2Ph$	PMe_3	Ph
2f, 3f	$SiMe_2Ph$	PEt_3	Ph
2g, 3g	$SiMe_2Ph$	$PMePh_2$	Ph
2h, 3h	$SiMe_2Ph$	PMe_2Ph	*p*-$H_2NC_6H_4$
2i, 3i	$SiMe_2Ph$	PMe_2Ph	*p*-MeC_6H_4
2j, 3j	$SiMe_2Ph$	PMe_2Ph	*p*-$OHCC_6H_4$

trans to the silyl ligands involve relatively small $^1J_{PtP}$ values (1419−1663 Hz), whereas those trans to the $SnMe_3$ ligand exhibit $^1J_{PtP}$ values of 2318−2513 Hz. The coalescence temperatures (T_c) vary significantly with the sorts of silyl and phosphine ligands. Thus, T_c rises according to the silyl ligands in the order $SiMe_3$ (**1a**) < $SiMe_2Ph$ (**1b**) < $SiMePh_2$ (**1c**) < $SiPh_3$ (**1d**) and according to the phosphine ligands in the order PEt_3 (**1f**) ≈ $PMePh_2$ (**1g**) < PMe_2Ph (**1b**) < PMe_3 (**1e**). The observed orders seem to reflect a delicate balance of electronic and steric effects.

Alkyne Insertion into *cis*-Pt(SiR_3)($SnMe_3$)L_2. Complexes **1** reacted with alkynes in solution to give two types of products, **2** and **3**, which are formed by the insertion into Pt−Sn and Pt−Si bonds, respectively (Scheme 4). The ratio of **2** to **3** varied significantly with the types of silyl and phosphine ligands, alkynes employed, and reaction conditions. As described below in detail, two types of processes are operative. One is competitive formation of **2** and **3**, and the other is subsequent conversion of **2** to **3**.

(a) Reaction of 1d with Phenylacetylene. Complex **1d** rapidly reacted with phenylacetylene (10 equiv) in $CDCl_3$ at 50 °C to give the insertion complex into the Pt−Si bond (**3d**), selectively. On the other hand, the same reaction examined in the presence of 1 equiv/**1d** of added PMe_2Ph proceeded gradually at the same temperature to afford a mixture of **3d** and **2d**, the latter of which is the insertion complex into the Pt−Sn bond. Figure 3a shows the time course. It is seen that **2d** and **3d** are simultaneously formed at the expense of **1d**. The ratio of **2d** to **3d** remains almost constant (93/7) during the reaction. Conversion of **1d** obeyed good pseudo-first-order kinetics up to 80% conversion (k_{obsd} = 1.02(2) × 10^{-4} s^{-1}).

When the amount of added PMe_2Ph was reduced to 0.1 equiv/**1d**, the insertion reaction proceeded much more rapidly (see Figure 3b). Furthermore, **2d** once formed in the reaction system was subsequently converted to **3d**. Thus, the amount of **2d** reaches the maximum (69%) after 20 min and then decreases with increasing amount of **3d**. The initial ratio of **2d** to **3d** is 93/7, and this value is in good agreement with that observed for Figure 3a.

(8) (a) Obora, Y.; Tsuji, Y.; Nishiyama, K.; Ebihara, M.; Kawamura, T. *J. Am. Chem. Soc.* **1996**, *118*, 10922. (b) Tsuji, Y.; Nishiyama, K.; Hori, S.; Ebihara, M.; Kawamura, T. *Organometallics* **1998**, *17*, 507. (c) Tsuji, Y.; Obora, Y. *J. Organomet. Chem.* **2000**, *611*, 343. (d) Wendt, O. F.; Deeth, R. J.; Elding, L. I. *Inorg. Chem.* **2000**, *39*, 5271.

Table 1. $^{31}P\{^1H\}$ NMR Data for *cis*-Pt(SiR_3)($SnMe_3$)L_2 (1a−g)[a]

complex	SiR_3	L	δ (ppm)	$^2J_{PP}$ (Hz)	$^1J_{PtP}$ (Hz)	$^2J_{^{119}SnP}$ (Hz)	$^2J_{^{117}SnP}$ (Hz)	T_c (°C)
1a	$SiMe_3$	PMe_2Ph	−5.3 (d)	28	1419	196	192	−15
			−5.7 (d)	28	2392	1634	1577	
1b	$SiMe_2Ph$	PMe_2Ph	−6.1 (d)	26	1526	194	184	5
			−8.3 (d)	26	2379	1616	1544	
1c	$SiMePh_2$	PMe_2Ph	−6.4 (d)	25	1606	187	181	15
			−9.8 (d)	25	2352	1561	1510	
1d	$SiPh_3$	PMe_2Ph	−5.4 (d)	25	1663	185	177	35
			−9.7 (d)	25	2331	1559	1449	
1e	$SiMe_2Ph$	PMe_3	−15.1 (d)	27	1464	201	193	20
			−17.8 (d)	27	2318	1645	1521	
1f	$SiMe_2Ph$	PEt_3	14.5 (br,d)	23	1629	185[b]		−30
			13.6 (br,d)	23	2513	1616[b]		
1g	$SiMe_2Ph$	$PMePh_2$	9.3 (br,d)	21	1596	197[b]		−25
			6.2 (br,d)	21	2461	1540[b]		

[a] In CD_2Cl_2, at −50 °C. [b] The $^2J_{^{119}SnP}$ and $^2J_{^{117}SnP}$ values were not resolved due to broadening of the satellite signals.

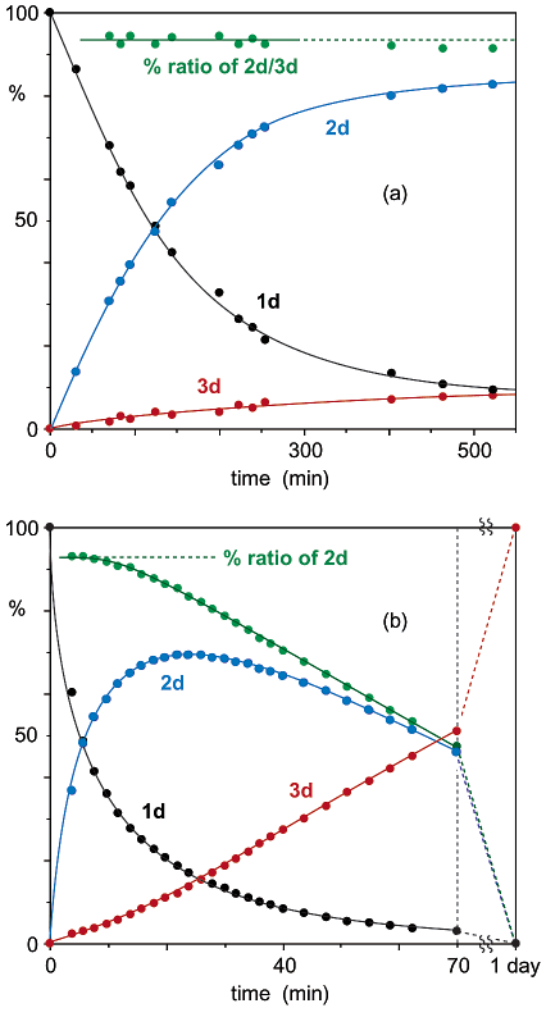

Figure 3. Time course of the reaction of **1d** with phenylacetylene in $CDCl_3$ in the presence of added PMe_2Ph at 50 °C. Initial concentration: $[\mathbf{1d}]_0 = 20$ mM, [PhC≡CH] = 0.20 M, $[PMe_2Ph]_0 = 20$ (a) or 2.0 mM (b).

The following points have emerged: (1) Insertion reactions into the Pt−Sn and Pt−Si bonds compete with each other under kinetic conditions, giving a 93/7 ratio of **2d** and **3d** at 50 °C. (2) Complex **2d** is entirely converted to **3d** under thermodynamic conditions. (3) Both processes are retarded by addition of free PMe_2Ph to the system.

Complex **3d** was isolated as a white crystalline solid and identified by NMR spectroscopy and elemental analysis. Although **2d** was not isolated owing to the occurrence of its conversion to **3d**, the formation of this complex was clearly confirmed by ^1H, $^{13}C\{^1H\}$, and $^{31}P\{^1H\}$ NMR spectroscopy. Figures 1b and 1c show the $^{31}P\{^1H\}$ NMR spectra of **2d** and **3d**, respectively. The site of phenylacetylene insertion (i.e., Pt−Sn or Pt−Si bond) could be confirmed with these spectra. Thus, **2d** exhibits two sets of doublets with ^{195}Pt satellites at δ −10.9 ($^1J_{PtP}$ = 1324 Hz) and −15.5 ($^1J_{PtP}$ = 1889 Hz). The $^1J_{PtP}$ values are comparable to those of *cis*-Pt($SiPh_3$){C(Ph)=CH($SiPh_3$)}(PMe_2Ph)$_2$ (1246 and 1820 Hz),[2b] *cis*-Pt($SiPh_3$)-{CH=CH($SiPh_3$)}(PMe_2Ph)$_2$ (1390 and 1821 Hz),[2b] and *cis*-Pt($SiPh_3$)(CH=CH_2)(PMe_2Ph)$_2$ (1342 and 1988 Hz).[2a] The occurrence of the insertion into the Pt−Sn bond is also supported by the absence of P−Sn couplings in the signals. In contrast, the signals of **3d** in Figure 1c involve the satellites due to the coupling to ^{117}Sn and ^{119}Sn nuclei, in addition to the ^{195}Pt satellites. The $^1J_{PtP}$ values (2081 and 1975 Hz) observed for **3d** are consistent with a structure having stannyl and alkenyl ligands in mutually cis positions.

The regiochemistry of phenylacetylene insertion giving the structures "Pt−C(Ph)=CH−($SnMe_3$)" in **2d** and "Pt−C(Ph)=CH($SiPh_3$)" in **3d** was confirmed by ^{13}C NMR spectroscopy. The α-vinylic carbon signal of **2d** appeared at δ 169.4 (dd, $^2J_{PC}$ = 99 and 17 Hz) with a large coupling to ^{195}Pt ($^1J_{PtC}$ = 713 Hz), and this signal vanished in a DEPT NMR spectrum because of the absence of a proton on this carbon. Similarly, the α-carbon signal of **3d** at δ 184.3 (dd, $^2J_{PC}$= 101 and 13 Hz, $^1J_{PtC}$ = 719 Hz) disappeared in a DEPT NMR spectrum.

(b) Effect of Silyl and Phosphine Ligands. Reactions of **1a**−**g** with phenylacetylene were similarly examined in the presence of 0.1 equiv/**1** of added phosphines (Table 2). The reaction of **1a** was complete in a few minutes even at −70 °C, giving the insertion complex into the Pt−$SiMe_3$ bond (**3a**), selectively (run 1). Complexes **1b** and **1e**−**g**, bearing a $SiMe_2Ph$ ligand, reacted with phenylacetylene at −5 °C to give kinetic mixtures of **2** and **3**, respectively (runs 2, 5−7); the ratios of **2** to **3** were unchanged at this temperature but converged to **3** at room temperature. Complexes **1c** and **1d** were less reactive and underwent insertion of phenylacetylene at elevated temperatures (runs 3, 4). As already shown for **1d** (Figure 3b), these systems involved competitive formation of **2** and **3** and subsequent conversion of **2** to **3**.

Table 2. Reactions of 1a−g with Phenylacetylene[a]

run	complex	SiR_3	L	reaction temp (°C)	10^3k_{obsd}[b] (s^{-1})	**2**:**3**[c]
1	**1a**	$SiMe_3$	PMe_2Ph	−70	rapid	0:100
2	**1b**	$SiMe_2Ph$	PMe_2Ph	−5	1.50(1)	30:70
3	**1c**	$SiMePh_2$	PMe_2Ph	15	0.326(3)	59:41
4[d]	**1d**	$SiPh_3$	PMe_2Ph	50	1.2(1)	93:7
5	**1e**	$SiMe_2Ph$	PMe_3	−5	2.4(1)	36:64
6	**1f**	$SiMe_2Ph$	PEt_3	−5	0.413(2)	25:75
7	**1g**	$SiMe_2Ph$	$PMePh_2$	−5	0.801(1)	25:75

[a] Reactions were performed in CD_2Cl_2 in the presence of added phosphines (L) unless otherwise noted. Initial concentration: $[\mathbf{1}]_0 = 20$ mM, $[PhC{\equiv}CH]_0 = 0.20$ M, $[L]_0 = 2.0$ mM. [b] Rate constants for the conversion of **1**, estimated by least-squares treatment of first-order plots at least for two half-lives. [c] The ratio of insertion products under kinetic conditions. [d] In $CDCl_3$.

Table 3. Reactions of 1b with Several Alkynes[a]

run	alkyne	10^3k_{obsd} (s^{-1})[b]	**2**:**3**[c]
1	*p*-$H_2NC_6H_4C{\equiv}CH$	1.20(2)	12:88
2	*p*-$MeC_6H_4C{\equiv}CH$	1.24(3)	28:72
3	$PhC{\equiv}CH$	1.50(1)	30:70
4	*p*-$OHCC_6H_4C{\equiv}CH$	rapid	46:54
5	$MeO_2CC{\equiv}CCO_2Me$	rapid	100:0

[a] Reactions were performed in CD_2Cl_2 at −5 °C in the presence of added PMe_2Ph. Initial concentration: $[\mathbf{1b}]_0 = 20$ mM, $[alkyne]_0 = 0.20$ M, $[PMe_2Ph]_0 = 2.0$ mM. [b] Rate constants for the conversion of **1b**, estimated by least-squares treatment of first-order plots at least for two half-lives. [c] The ratio of insertion products under kinetic conditions.

Table 2 suggests the following points: (1) The reactivity of **1** decreases according to silyl and phosphine ligands in the order $SiMe_3$ (**1a**) > $SiMe_2Ph$ (**1b**) > $SiMePh_2$ (**1c**) > $SiPh_3$ (**1d**); PMe_3 (**1e**) > PMe_2Ph (**1b**) > $PMePh_2$ (**1g**) > PEt_3 (**1f**). (2) The kinetic ratio of **2** to **3** increases according to silyl ligands [$SiMe_3$ (**1a**) < $SiMe_2Ph$ (**1b**) < $SiMePh_2$ (**1c**) < $SiPh_3$ (**1d**)] and to phosphine ligands [PEt_3 (**1f**) = $PMePh_2$ (**1g**) < PMe_2Ph (**1b**) ≈ PMe_3 (**1e**)]. The effect of silyl ligands is particularly remarkable, and the kinetic ratio varies from 0/100 to 93/7.

(c) Effect of Alkynes. Table 3 compares the reactions of **1b** with several acetylenes in CD_2Cl_2 at −5 °C. It is seen that the acetylene bearing more electron-withdrawing substituent(s) tends to give a higher reactivity and a higher kinetic ratio of **2**. The mixtures of insertion products formed in runs 1−4 were entirely converted to **3** at room temperature. On the other hand, **2k**, formed by the insertion of dimethyl acetylenedicarboxylate into the Pt−Sn bond of **1b**, was exceptionally stable and isolated as a crystalline solid suitable for X-ray diffraction analysis.

Figure 4 shows the ORTEP diagram of **2k**. The complex adopts square-planar geometry; the sum of the four angles around platinum is 360.0°. The Pt−P(1) bond (2.377(2) Å) is significantly longer than the Pt−P(2) bond (2.306(2) Å), reflecting the difference in trans influence of silyl and alkenyl ligands. The $SnMe_3$ group is bonded to the *β*-vinylic carbon in cis orientation toward platinum, showing the occurrence of cis insertion of dimethyl acetylenedicarboxylate into the Pt−Sn bond of **1b**.

(d) Kinetic Study. The reaction progress of **1b** with phenylacetylene in CD_2Cl_2 at −5.0 °C was followed by ^1H NMR spectroscopy at several concentrations of $PhC{\equiv}CH$ and added PMe_2Ph. Figure 5a shows a representative example of the time course. Complexes **2b** and **3b** are simultaneously formed in the ratio of 30/70 throughout the reaction. The conversion of **1b** obeys good pseudo-first-order kinetics at least for two half-lives under the conditions using an excess amount of phenylacetylene (see Figure 5b).[9]

Table 4 lists the rate constants observed under various conditions. The reaction proceeded more rapidly

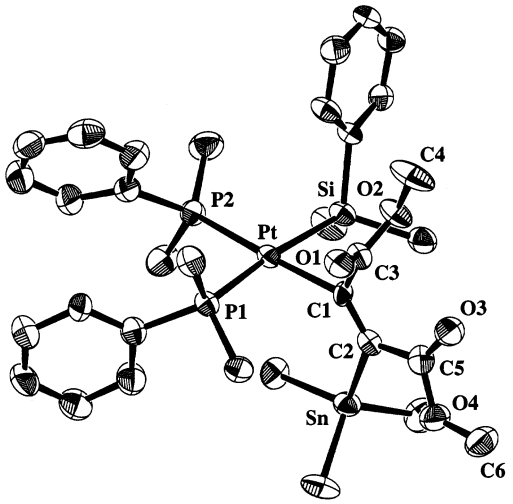

Figure 4. X-ray structure of **2k**. Hydrogen atoms are omitted for clarity. Selected bond distances (Å) and angles (deg): Pt−Si = 2.394(2), Pt−P(1) = 2.377(2), Pt−P(2) = 2.306(2), Pt−C(1) = 2.099(6), C(1)−C(2) = 1.30(1), C(1)−C(3) = 1.52(1), C3(1)−O(1) = 1.195(8), C(3)−O(2) = 1.328-(8), O(2)−C(4) = 1.449(9), C(2)−Sn = 2.168(6), C(2)−C(5) = 1.480(9), C(5)−O(3) = 1.220(8), C(5)−O(4) = 1.373(9), O(4)−C(6) = 1.42(1), Si−Pt−C(1) = 83.9(2), P(1)−Pt−P(2) = 96.42(6), Si−Pt−P(1) = 172.20(6), Si−Pt−P(2) = 91.34-(7), P(1)−Pt−C(1) = 88.3(2), P(2)−Pt−C(1) = 175.2(2), Pt−C(1)−C(2) = 128.9(6), Pt−C(1)−C(3) = 107.9(5), C(2)−C(1)−C(3) = 123.1(6), Sn−C(2)−C(1) = 127.4(5), Sn−C(2)−C(5) = 114.0(5), C(1)−C(2)−C(5) = 118.5(6), O(1)−C(3)−O(2) = 125.0(6), O(1)−C(3)−C(1) = 123.1(6), O(2)−C(3)−C(1) = 111.8(5), O(3)−C(5)−O(4) = 120.0(6), O(3)−C(5)−C(2) = 129.0(7), O(4)−C(5)−C(2) = 111.0(6), C(3)−O(2)−C(4) = 114.1(6), C(5)−O(4)−C(6) = 118.0(6).

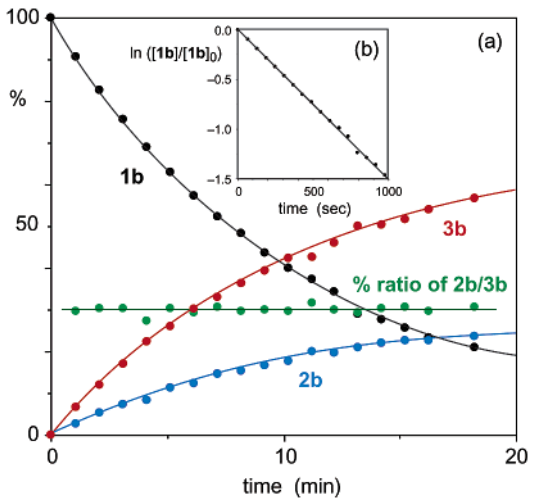

Figure 5. Time course of the reaction of **1b** with phenylacetylene in CD_2Cl_2 in the presence of added PMe_2Ph at −5.0 °C (plot a). Initial concentration: $[\mathbf{1b}]_0 = 20$ mM, $[PhC{\equiv}CH] = 0.20$ M, $[PMe_2Ph]_0 = 2.0$ mM. Plot b represents the first-order plot for the conversion of **1b**.

Table 4. Kinetic Data for the Reaction of 1b with Phenylacetylene

run[a]	$[PhC{\equiv}CH]_0$ (M)	$[PMe_2Ph]_0$ (mM)	10^3k_{obsd} (s^{-1})[b]
1	0.20	2.0	1.50(1)
2	0.15	2.5	0.755(1)
3	0.20	2.5	1.15(1)
4	0.30	2.5	1.75(2)
5	0.58	2.5	3.14(3)
6	0.30	15	0.595(1)
7	0.30	22	0.455(1)
8	0.30	30	0.324(1)

[a] All runs were performed in CD_2Cl_2 at −5.0 °C in the presence of added PMe_2Ph. Initial concentration: $[\mathbf{1b}]_0 = 20$ (run 1) or 25 mM (runs 2−8). [b] Rate constants for the conversion of **1b**, estimated by least-squares treatment of first-order plots at least for two half-lives.[9]

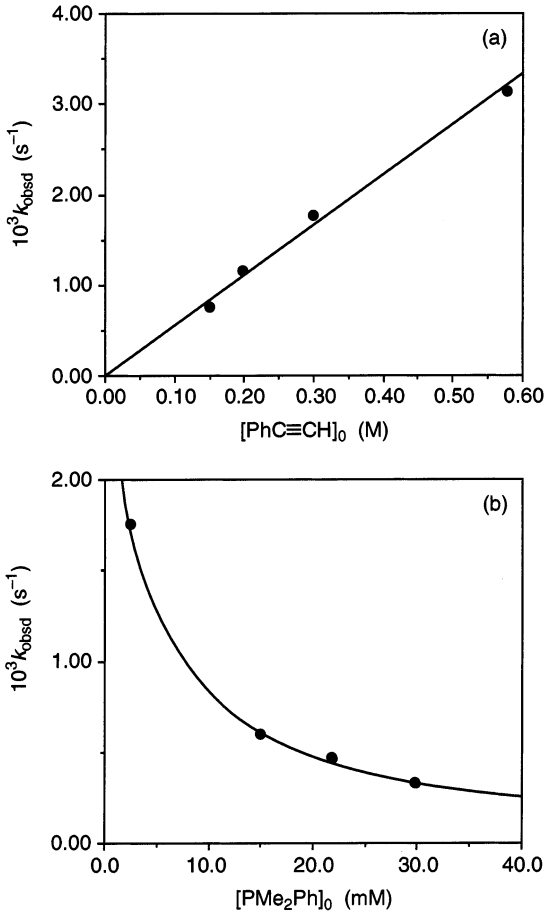

Figure 6. (a) Plot of pseudo-first-order rate constants against phenylacetylene concentration for the data of runs 2−5 in Table 4. (b) Plot of pseudo-first-order rate constants against concentration of added PMe_2Ph for the data of runs 4 and 6−8 in Table 4.

at higher concentration of phenylacetylene (runs 2−5). The plot of k_{obsd} against $[PhC{\equiv}CH]_0$ gave a straight line including the origin (Figure 6a). On the other hand, the reaction was retarded by addition of free PMe_2Ph to the system (runs 4 and 6−8, and Figure 6b).

(e) Conversion of 2 to 3. We have described that **2** formed under kinetic conditions is subsequently converted to **3** under thermodynamic conditions. This reaction is clearly retarded by addition of free phosphine to the system. Furthermore, the following crossover experiments have suggested an intramolecular process for the conversion. Thus, the kinetic mixture of **2b** and **3b** (30/70), generated in situ from **1b** and PhC≡CH (1 equiv) in CD_2Cl_2 in the presence of free PMe_2Ph (0.1 equiv) at −5 °C, was treated with *p*-$MeC_6H_4C{\equiv}CH$ (3 equiv) at 35 °C for 3 h (Scheme 5). NMR examination of the resulting reaction solution revealed selective conversion of **2b** to **3b**; no trace of the insertion product of *p*-$MeC_6H_4C{\equiv}CH$ (**3i**) was detected. Similarly, heating a kinetic mixture of **2i** and **3i** (28/72) with PhC≡CH (3 equiv) in CD_2Cl_2 at 35 °C for 3 h led to selective formation of **3i**.

Scheme 5[a]

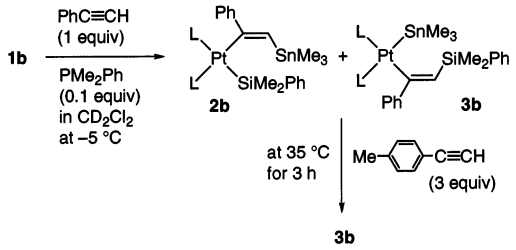

[a] L = PMe_2Ph.

Discussion

Mechanism of Alkyne Insertion. The kinetic observations for **1b** are consistent with the insertion mechanism given in Scheme 6. The first step is associative displacement of one of the phosphine ligands (L) in **1** with alkyne to give **4** and **5**, which are very probably interconverted with each other by twist-rotation similarly to **1** (Scheme 3). The rate of twist-rotation for **1b** was estimated to be 1.8×10^2 s^{-1} at −5 °C by line-shape analysis of the $^{31}P\{^1H\}$ NMR spectrum, and this value is about 10^5 greater than the rate of phenylacetylene insertion into **1b**. Although we had no direct information about the rate of interconversion between **4** and **5**, all phenomena observed in this study have been found to be reasonably interpreted by assuming the occurrence of rapid equilibrium between these intermediates (vide infra).

Complexes **4** and **5** undergo migratory insertion in the next step. Stannyl migration in **4** gives a three-coordinate intermediate **6**, which is subsequently converted to **2** by trans-to-cis isomerization followed by coordination of L. On the other hand, silyl migration in **5** causes the formation of **3** via the intermediate **7**.

When the interconversion between **4** and **5** is rapid enough to keep the ratio of **4** to **5** constant, and the steady-state approximation can be applied to the total concentration of **4** and **5**, the following relation holds:

$$(k_{1Sn} + k_{1Si})[R'C{\equiv}CH][\mathbf{1}] = (k_{-1Sn}[\mathbf{4}] + k_{-1Si}[\mathbf{5}])[L] + (k_{2Sn}[\mathbf{4}] + k_{2Si}[\mathbf{5}]) \quad (1)$$

Since $[\mathbf{5}] = K[\mathbf{4}]$,

$$(k_{1Sn} + k_{1Si})[R'C{\equiv}CH][\mathbf{1}] = \{(k_{-1Sn} + k_{-1Si}K)[L] + (k_{2Sn} + k_{2Si}K)\}[\mathbf{4}] \quad (2)$$

(9) The k_{obsd} values of runs 2 and 3 in Table 4 were derived from the first-order plots of the data up to 58% and 76% conversion of **1b**, respectively.

Scheme 6

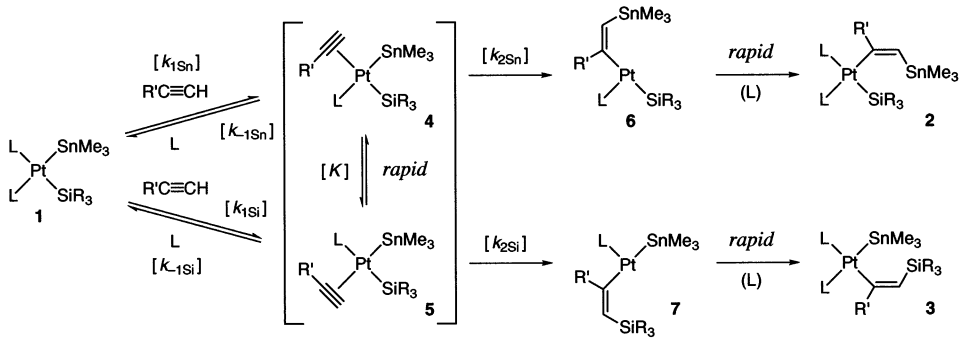

Accordingly,

$$[\mathbf{4}] = \frac{(k_{1Sn} + k_{1Si})[R'C{\equiv}CH]}{(k_{-1Sn} + k_{-1Si}K)[L] + (k_{2Sn} + k_{2Si}K)}[\mathbf{1}] \quad (3)$$

On the other hand, if the conversions of **6** to **2** and **7** to **3** are sufficiently faster than the migratory insertion in **4** and **5**, the sum of the formation rates of **2** and **3** (i.e., the rate of conversion of **1**) can be expressed as follows:

$$\frac{d[\mathbf{2}]}{dt} + \frac{d[\mathbf{3}]}{dt} = -\frac{d[\mathbf{1}]}{dt} = k_{2Sn}[\mathbf{4}] + k_{2Si}[\mathbf{5}] = (k_{2Sn} + k_{2Si}K)[\mathbf{4}] \quad (4)$$

Substitution of eq 3 into eq 4 yields the following rate expression:

$$-\frac{d[\mathbf{1}]}{dt} = \frac{(k_{1Sn} + k_{1Si})(k_{2Sn} + k_{2Si}K)[R'C{\equiv}CH]}{(k_{-1Sn} + k_{-1Si}K)[L] + (k_{2Sn} + k_{2Si}K)}[\mathbf{1}] \quad (5)$$

Thus, the k_{obsd} value is correlated with the concentrations of R′C≡CH and L by the following equation:

$$\frac{[R'C{\equiv}CH]}{k_{obsd}} = \frac{(k_{-1Sn} + k_{-1Si}K)[L]}{(k_{1Sn} + k_{1Si})(k_{2Sn} + k_{2Si}K)} + \frac{1}{(k_{1Sn} + k_{1Si})} \quad (6)$$

Figure 7 shows the plot of $[PhC{\equiv}CH]_0/k_{obsd}$ values against $[PMe_2Ph]_0$ values for all runs in Table 4, giving a good linear correlation ($r = 0.998$) fully consistent with eq 6. Based on the intercept and slope, the $(k_{1Sn} + k_{1Si})$ and $(k_{-1Sn} + k_{-1Si}K)/(k_{2Sn} + k_{2Si}K)$ values were estimated as $0.94(1) \times 10^{-2}$ s^{-1} M^{-1} and $2.5(1) \times 10^2$, respectively.

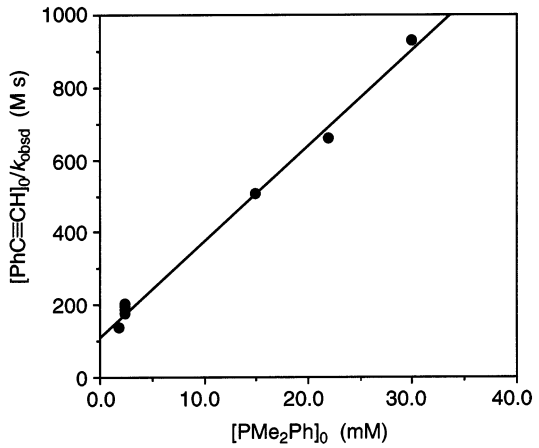

Figure 7. Plot of $[PhC{\equiv}CH]_0/k_{obsd}$ values against $[PMe_2Ph]_0$ values for all data in Table 4.

Effect of Silyl and Phosphine Ligands. (a) Reaction Rate. Based on the kinetic analysis described above, the overall rate of the conversion of **1** to **2** and **3** is considered to be controlled at two stages. One is associative displacement of one of the phosphine ligands in **1** with alkyne, and the other is migratory insertion of the alkyne ligands in **4** and **5** into Pt−Sn and Pt−Si bonds, respectively. As seen from Table 2, variation in the rate constants is particularly remarkable for the change of silyl ligands. This tendency is rationalized by assuming the latter stage to be more crucial for controlling the reaction rate, and this assumption is consistent with the balance of the rate constants for **1b**: $(k_{-1Sn} + k_{-1Si}K)/(k_{2Sn} + k_{2Si}K) = 2.5(1) \times 10^2$. Thus, reflecting increase in Pt−Si bond energy,[10] the rate of migratory insertion in **5** may be reduced in the order $SiMe_3$ (**1a**) > $SiMe_2Ph$ (**1b**) > $SiMePh_2$ (**1c**) > $SiPh_3$, causing a drop in the overall rate. As we discuss later, this point is also related to the marked dependence of the kinetic ratio of **2** to **3** on silyl ligands.

The data in Table 2 also suggest that bulkiness of silyl and phosphine ligands serves as another factor to control the reactivity. Thus, it seems reasonable that bulky ligands prevent the association of alkyne with **1** to retard the formation of **4** and **5**, although the possibility that the rates of migratory insertion in **4** and **5** are also reduced by steric factors cannot be excluded.

(b) Kinetic Ratio. The kinetic ratio of **2** to **3** may be dictated by two factors. One is the ratio of **4** to **5**, and the other is the relative rates of migratory insertion (i.e., k_{2Sn} vs k_{2Si}). As seen from the data of runs 1−4 in Table 2, the kinetic ratio of **2** to **3** remarkably increases in the order **1a** < **1b** < **1c** < **1d**. Since these complexes have the same ligands except for silyl ligands, the dramatic change in the kinetic ratio is attributed to the nature of silyl ligands.

As for the equilibrium between **4** and **5**, the highly electron-releasing $SiMe_3$ ligand may coordinate most preferentially to the position trans to the alkyne ligand in **4**, rather than the position trans to the phosphine ligand in **5**, to reduce electronic repulsion between trans ligands. On the other hand, the bulky $SiPh_3$ ligand will be most favorably accommodated at the position cis to the alkyne ligand in **5**, rather than the position cis to the phosphine ligand in **4**, to avoid steric hindrance

(10) Generally, electron-withdrawing substituents on silicon lead to strengthening of Pt−Si bonds: (a) Sakaki, S.; Mizoe, N.; Sugimoto, M. *Organometallics* **1998**, *17*, 2510. (b) Sakaki, S.; Mizoe, N.; Sugimoto, M.; Musashi, Y. *Coord. Chem. Rev.* **1999**, *190−192*, 933.

between the silyl and phosphine ligands. Accordingly, the ratio of **4** to **5** is expected to decrease in the order $SiMe_3$ (**1a**) > $SiMe_2Ph$ (**1b**) > $SiMePh_2$ (**1c**) > $SiPh_3$ (**1d**) from both electronic and steric viewpoints. Since this order is just the reverse of the sequence of kinetic ratios actually observed, the marked variation in the kinetic ratios for **1a**−**d** must be considered to mainly reflect the other factor, i.e., the difference in the insertion rates in **4** and **5**. Since the Pt−Si bond becomes stronger in the order $SiMe_3$ (**1a**) < $SiMe_2Ph$ (**1b**) < $SiMePh_2$ (**1c**) < $SiPh_3$ (**1d**),[10] the rate of migratory insertion in **5** should be reduced in this order, and as a result, the product ratio of **2** increases.

Comparing the product ratios for runs 2 and 5−7 in Table 2, there is a tendency that the ratio of **3** increases as the phosphine ligand becomes bulkier. Since the complexes employed in these runs (**1b** and **1e**−**g**) have the same silyl and stannyl ligands, it seems likely that all complexes adopt a very similar balance of migratory insertion rates. Consequently, the modest variation in the product ratio is attributable mainly to a change in the equilibrium position between **4** and **5** dependent on the bulkiness of phosphine ligands. As already seen for the X-ray structure of **1d**, the Pt−Sn bond is more flexible than the Pt−Si bond. Moreover, the Pt−Sn bond is significantly longer than the Pt−Si bond. Therefore, it is likely that steric hindrance takes place more remarkably between the silyl and phosphine ligands than between the stannyl and phosphine ligands. This situation causes shift of the equilibrium position toward **5** as the phosphine ligand becomes bulkier, and hence the kinetic ratio of **3** increases.

Effect of Alkynes. A dramatic change in the kinetic ratio of **2** to **3** has also been noted for the insertion of five kinds of alkynes into **1b** (Table 3). Thus, more electron-deficient alkynes tend to insert more preferably into the Pt−Sn bond. Since the overall rate of the insertion is enhanced at the same time, it is considered that electron-deficient alkynes mainly accelerate the insertion into the Pt−Sn bond.

As already pointed out for a related palladium system,[4a] the insertion into the Pt−Sn bond may be disadvantageous over the insertion into the Pt−Si bond in a thermodynamic sense because the C−Sn bond generated in the former process is weaker than the C−Si bond formed in the latter process. However, when the Pt−C bond simultaneously formed in the alkyne insertion is sufficiently strong to compensate the energetically unfavorable situation associated with the weaker C−Sn bond, the relative ease of the insertions in **4** and **5** may be reversed by a kinetic reason originating from the weaker Pt−Sn bond than the Pt−Si bond, which makes the migration of the $SnMe_3$ group easier than that of the $SiMe_2Ph$ group. The results in Table 3 should be the case where more electron-withdrawing substituents provide stronger Pt−C bonds in the insertion complexes.

Mechanism of the Conversion of 2 to 3. It has been suggested that the conversion of **2** to **3** proceeds via an intramolecular process involving phosphine dissociation. Scheme 7 illustrates our proposed mechanism. As seen from the X-ray structure of **2k** in Figure 4, the alkenyl ligand in **2** is perpendicularly oriented toward the coordination plane to avoid steric hindrance to silyl

Scheme 7

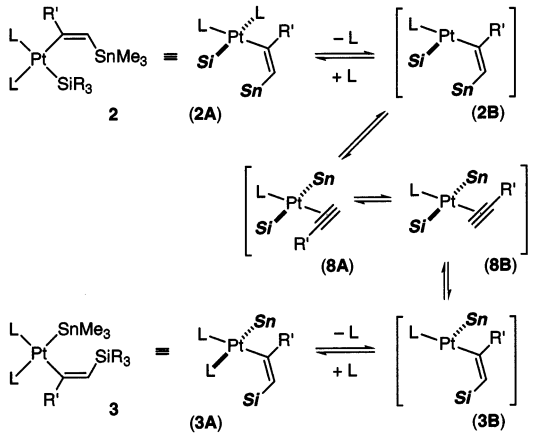

and phosphine ligands (**2A**). Dissociation of phosphine followed by β-stannyl group elimination from the resulting **2B** forms an alkyne-coordinated silyl(stannyl) intermediate (**8A**), which is in an equilibrium with **8B** as a rotational isomer of the alkyne ligand. Migration of the silyl group on the alkyne ligand in **8B** affords **3B**, which undergoes phosphine coordination to give **3A** (= **3**). It should be noted that intermediates **8A** and **8B** have the silyl and stannyl ligands in mutually trans positions, and they are different from **4** and **5** in Scheme 6. Accordingly, the conversion of **2** into **3** under thermodynamic conditions is operative independent of the alkyne insertion into **1** under kinetic conditions.

Conclusions

We have succeeded for the first time in observing details of the alkyne insertion into *cis*-silyl(stannyl)-platinum(II) complexes having two tertiary phosphine ligands (**1**). The reactions consist of competitive insertion of alkynes into the Pt−Sn and Pt−Si bonds, giving the corresponding insertion complexes **2** and **3**, respectively, and the subsequent conversion of **2** to **3** as thermodynamic products. The ratio of **2** to **3** under kinetic conditions is significantly affected by the types of silyl and phosphine ligands and alkynes employed. The variations thus observed have been reasonably interpreted on the basis of the insertion mechanism involving associative displacement of one of the phosphine ligands in **1** with alkynes, followed by competitive migration of the stannyl and silyl ligands on the alkyne ligand in the resulting **4** and **5**, which are rapidly interconverting with each other under reaction conditions (Scheme 6).

Experimental Section

General Considerations. All manipulations were carried out under a nitrogen atmosphere using conventional Schlenk techniques. Nitrogen gas was dried by passage through P_2O_5 (Merck, SICAPENT). NMR spectra were recorded on a JEOL JNM-A400 or Varian Mercury 300 spectrometer. Chemical shifts are reported in δ (ppm) referenced to an external $SiMe_4$ standard for ^1H and ^{13}C NMR and to an external 85% H_3PO_4 standard for ^{31}P NMR. Et_2O, pentane, and THF were dried over sodium benzophenone ketyl and distilled prior to use. CH_2Cl_2 was dried over CaH_2 and distilled prior to use. CD_2Cl_2 was purified by passing through a short Al_2O_3 column and

stored under a nitrogen atmosphere. $Pt(cod)_2$ was prepared according to the literature.[11]

Preparation of *cis*-Pt(SiPh$_3$)(SnMe$_3$)(PMe$_2$Ph)$_2$ (1d). To a Schlenk tube containing $Pt(cod)_2$ (503 mg, 1.22 mmol) and $Ph_3SiSnMe_3$ (542 mg, 1.28 mmol) was added toluene (30 mL) at 0 °C under a nitrogen atmosphere. Addition of PMe_2Ph (337 mg, 2.44 mmol) to the system with stirring gave a reddish brown solution, a part of which was transferred into an NMR sample tube equipped with a rubber septum cap by cannulation and examined by $^{31}P\{^1H\}$ NMR spectroscopy, showing the quantitative formation of **1d**. The solution was stirred at room temperature for 1 h and then concentrated to almost dryness by pumping. Et_2O (3 mL) and pentane (5 mL) were added, and the resulting yellow-brown solid was collected by filtration, washed with pentane (2 mL × 3), and dried under vacuum. Recrystallization of the crude product from a mixture of THF and Et_2O gave yellow crystals of **1d**·THF, suitable for single-crystal X-ray diffraction study (450 mg, 38%).

Complex 1d. ^1H NMR (CD_2Cl_2, −50 °C): δ −0.42 (s, $^3J_{PtH}$ = 6.8 Hz, $^2J_{SnH}$ = 38.7 Hz, 9H, SnMe), 0.57 (d, $^2J_{PH}$ = 9.0 Hz, $^3J_{PtH}$ = 24.6 Hz, 6H, PMe), 1.27 (d, $^2J_{PH}$ = 7.8 Hz, $^3J_{PtH}$ = 19.8 Hz, 6H, PMe), 7.1−7.7 (m, 19H, Ph), 7.82 (d, $^3J_{HH}$ = 7.2 Hz, 6H, SiPh). $^{13}C\{^1H\}$ NMR (CD_2Cl_2, −50 °C): δ −3.4 (dd, $^3J_{PC}$ = 11 and 4 Hz, $^2J_{PtC}$ = 66 Hz, $^1J_{SnC}$ = 181 Hz, SnMe), 14.6 (dd, $^1J_{PC}$ = 26 Hz, $^3J_{PC}$ = 3 Hz, $^2J_{PtC}$ = 34 Hz, PMe), 17.0 (dd, $^1J_{PC}$ = 24 Hz, $^3J_{PC}$ = 4 Hz, $^2J_{PtC}$ = 25 Hz, PMe), 126.8 (s, SiPh), 127.0 (s, SiPh), 128.0 (d, $^3J_{PC}$ = 9 Hz, PPh), 129.3 (s, PPh), 129.7 (d, $^2J_{PC}$ = 10 Hz, PPh), 129.8 (d, $^2J_{PC}$ = 10 Hz, PPh), 136.6 (s, $^3J_{PtC}$ = 24 Hz, SiPh), 139.4 (dd, $^1J_{PC}$ = 40 Hz, $^3J_{PC}$ = 5 Hz, PPh), 139.9 (dd, $^1J_{PC}$ = 41 Hz, $^3J_{PC}$ = 6 Hz, PPh), 145.6 (t, $^3J_{PC}$ = 6 Hz, $^2J_{PtC}$ = 46 Hz, SiPh). $^{31}P\{^1H\}$ NMR (CD_2Cl_2, −50 °C): δ −5.4 (d, $^2J_{PP}$ = 25 Hz, $^1J_{PtP}$ = 1663 Hz, $^2J^{119}_{SnP}$ = 185 Hz, $^2J^{117}_{SnP}$ = 177 Hz), −9.7 (d, $^2J_{PP}$ = 25 Hz, $^1J_{PtP}$ = 2331 Hz, $^2J^{119}_{SnP}$ = 1559 Hz, $^2J^{117}_{SnP}$ = 1499 Hz). Anal. Calcd for $C_{37}H_{46}P_2SiSnPt{\cdot}C_4H_8O$: C, 50.94; H, 5.63. Found: C, 50.90; H, 5.42.

Complexes **1a**−**c**, **1f**, and **1g** were similarly obtained in 86% (**1a**), 56% (**1b**), 64% (**1c**), 78% (**1f**), and 74% (**1g**) yields, respectively. Complex **1e** was prepared by essentially the same procedure. Although the crude product contained a considerable amount of $Pt(cod)(PMe_3)_2$, this compound was removed by washing with Et_2O and pentane at room temperature. Recrystallization of the resulting product formed analytically pure **1e** (35%).

Complex 1a. ^1H NMR (CD_2Cl_2, −50 °C): δ 0.03 (s, $^3J_{PtH}$ = 6.9 Hz, $^2J_{SnH}$ = 36.3 Hz, 9H, SnMe), 0.20 (d, $^4J_{PH}$ = 2.4 Hz, $^3J_{PtH}$ = 22.8 Hz, 9H, SiMe), 1.51 (d, $^2J_{PH}$ = 6.6 Hz, $^3J_{PtH}$ = 18.6 Hz, 6H, PMe), 1.54 (d, $^2J_{PH}$ = 7.5 Hz, $^3J_{PtH}$ = 27.0 Hz, 6H, PMe), 7.1−7.8 (m, 10H, Ph). $^{13}C\{^1H\}$ NMR (CD_2Cl_2, −50 °C): δ −2.1 (dd, $^3J_{PC}$ = 11 and 5 Hz, $^2J_{PtC}$ = 76 Hz, $^1J_{SnC}$ = 181 Hz, SnMe), 9.0 (dd, $^3J_{PC}$ = 7 and 6 Hz, $^2J_{PtC}$ = 69 Hz, SiMe), 18.1 (dd, $^1J_{PC}$ = 26 Hz, $^3J_{PC}$ = 7 Hz, $^2J_{PtC}$ = 43 Hz, PMe), 18.7 (dd, $^1J_{PC}$ = 22 Hz, $^3J_{PC}$ = 7 Hz, $^2J_{PtC}$ = 30 Hz, PMe), 127.9 (d, $^3J_{PC}$ = 9 Hz, PPh), 127.9 (d, $^3J_{PC}$ = 8 Hz, PPh), 129.5 (s, PPh), 129.7 (s, PPh), 131.2 (d, $^2J_{PC}$ = 12 Hz, PPh), 131.4 (d, $^2J_{PC}$ = 11 Hz, PPh), 138.5 (dd, $^1J_{PC}$ = 37 Hz, $^3J_{PC}$ = 7 Hz, PPh), 139.1 (dd, $^1J_{PC}$ = 32 Hz, $^3J_{PC}$ = 6 Hz, PPh). $^{31}P\{^1H\}$ NMR (CD_2Cl_2, −50 °C): δ −5.3 (d, $^2J_{PP}$ = 28 Hz, $^1J_{PtP}$ = 1419 Hz, $^2J^{119}_{SnP}$ = 196 Hz, $^2J^{117}_{SnP}$ = 192 Hz), −5.7 (d, $^2J_{PP}$ = 28 Hz, $^1J_{PtP}$ = 2392 Hz, $^2J^{119}_{SnP}$ = 1634 Hz, $^2J^{117}_{SnP}$ = 1577 Hz). Anal. Calcd for $C_{22}H_{40}P_2SiSnPt$: C, 37.30; H, 5.69. Found: C, 37.65; H, 5.43.

Complex 1b. ^1H NMR (CD_2Cl_2, −50 °C): δ −0.01 (s, $^3J_{PtH}$ = 7.5 Hz, $^2J_{SnH}$ = 36.6 Hz, 9H, SnMe), 0.45 (d, $^4J_{PH}$ = 2.4 Hz, $^3J_{PtH}$ = 26.1 Hz, 6H, SiMe), 0.91 (d, $^2J_{PH}$ = 8.7 Hz, $^3J_{PtH}$ = 25.5 Hz, 6H, PMe), 1.30 (d, $^2J_{PH}$ = 7.5 Hz, $^3J_{PtH}$ = 18.6 Hz, 6H, PMe), 7.1−7.5 (m, 13H, Ph), 7.56 (d, $^3J_{HH}$ = 6.9 Hz, 2H, SiPh). $^{13}C\{^1H\}$ NMR (CD_2Cl_2, −50 °C): δ −2.5 (dd, $^3J_{PC}$ = 11 and 4 Hz, $^2J_{PtC}$ = 75 Hz, $^1J_{SnC}$ = 179 Hz, SnMe), 7.2 (dd, $^3J_{PC}$ = 8 and 5 Hz, $^2J_{PtC}$ = 76 Hz, SiMe), 15.6 (dd, $^1J_{PC}$ = 26 Hz, $^3J_{PC}$ = 4 Hz, $^2J_{PtC}$ = 41 Hz, PMe), 17.5 (d, $^1J_{PC}$ = 24 Hz, $^3J_{PC}$ = 4 Hz, $^2J_{PtC}$ = 25 Hz, PMe), 126.5 (s, SiPh), 126.8 (s, SiPh), 127.8 (d, $^3J_{PC}$ = 9 Hz, PPh), 127.9 (d, $^3J_{PC}$ = 9 Hz, PPh), 129.2 (s, PPh), 130.2 (dd, $^2J_{PC}$ = 10 Hz, $^3J_{PtP}$ = 16 Hz, PPh), 130.4 (dd, $^2J_{PC}$ = 11 Hz, $^3J_{PtP}$ = 13 Hz, PPh), 134.4 (s, $^3J_{PtC}$ = 17 Hz, SiPh), 139.4 (dd, $^1J_{PC}$ = 41 Hz, $^3J_{PC}$ = 7 Hz, PPh), 139.7 (dd, $^1J_{PC}$ = 37 Hz, $^3J_{PC}$ = 5 Hz, PPh), 151.6 (dd, $^3J_{PC}$ = 9 and 7 Hz, $^2J_{PtC}$ = 31 Hz, SiPh). $^{31}P\{^1H\}$ NMR (CD_2Cl_2, −50 °C): δ −6.1 (d, $^2J_{PP}$ = 26 Hz, $^1J_{PtP}$ = 1526 Hz, $^2J^{119}_{SnP}$ = 194 Hz, $^2J^{117}_{SnP}$ = 184 Hz), −8.3 (d, $^2J_{PP}$ = 26 Hz, $^1J_{PtP}$ = 2379 Hz, $^2J^{119}_{SnP}$ = 1616 Hz, $^2J^{117}_{SnP}$ = 1544 Hz). Anal. Calcd for $C_{27}H_{42}P_2SiSnPt$: C, 42.09; H, 5.49. Found: C, 41.95; H, 4.23.

Complex 1c. ^1H NMR (CD_2Cl_2, −50 °C): δ −0.19 (s, $^3J_{PtH}$ = 6.4 Hz, $^2J_{SnH}$ = 37.5 Hz, 9H, SnMe), 0.71 (d, $^2J_{PH}$ = 8.7 Hz, $^3J_{PtH}$ = 25.2 Hz, 6H, PMe), 0.81 (d, $^2J_{PH}$ = 2.4 Hz, $^3J_{PtH}$ = 30.6 Hz, 6H, SiMe), 1.26 (d, $^2J_{PH}$ = 7.8 Hz, $^3J_{PtH}$ = 18.6 Hz, 6H, PMe), 7.1−7.5 (m, 16H, Ph), 7.63 (d, $^3J_{HH}$ = 6.6 Hz, 4H, SiPh). $^{13}C\{^1H\}$ NMR (CD_2Cl_2, −50 °C): δ −2.7 (dd, $^3J_{PC}$ = 11 and 4 Hz, $^2J_{PtC}$ = 71 Hz, $^1J_{SnC}$ = 178 Hz, SnMe), 6.0 (dd, $^3J_{PC}$ = 7 and 3 Hz, $^2J_{PtC}$ = 82 Hz, SiMe), 15.4 (dd, $^1J_{PC}$ = 26 Hz, $^3J_{PC}$ = 3 Hz, $^2J_{PtC}$ = 36 Hz, PMe), 17.5 (dd, $^1J_{PC}$ = 24 Hz, $^3J_{PC}$ = 4 Hz, $^2J_{PtC}$ = 25 Hz, PMe), 127.0 (s, SiPh), 128.1 (d, $^3J_{PC}$ = 8 Hz, PPh), 130.1 (d, $^2J_{PC}$ = 10 Hz, PPh), 130.2 (d, $^2J_{PC}$ = 11 Hz, PPh), 135.5 (s, $^3J_{PtC}$ = 19 Hz, SiPh), 139.9 (dd, $^1J_{PC}$ = 38 Hz, $^3J_{PC}$ = 5 Hz, PPh), 140.1 (dd, $^1J_{PC}$ = 42 Hz, $^3J_{PC}$ = 7 Hz, PPh), 149.0 (t, $^3J_{PC}$ = 7 Hz, $^2J_{PtC}$ = 40 Hz, SiPh). $^{31}P\{^1H\}$ NMR (CD_2Cl_2, −50 °C): δ −6.4 (d, $^2J_{PP}$ = 25 Hz, $^1J_{PtP}$ = 1606 Hz, $^2J^{119}_{SnP}$ = 187 Hz, $^2J^{117}_{SnP}$ = 181 Hz), −9.8 (d, $^2J_{PP}$ = 25 Hz, $^1J_{PtP}$ = 2352 Hz, $^2J^{119}_{SnP}$ = 1561 Hz, $^2J^{117}_{SnP}$ = 1510 Hz). Anal. Calcd for $C_{32}H_{44}P_2SiSnPt$: C, 46.17; H, 5.33. Found: C, 45.93; H, 5.13.

Complex 1e. ^1H NMR (CD_2Cl_2, −50 °C): δ −0.01 (s, $^3J_{PtH}$ = 6.6 Hz, $^2J_{SnH}$ = 36.0 Hz, 9H, SnMe), 0.40 (d, $^4J_{PH}$ = 2.7 Hz, $^3J_{PtH}$ = 25.2 Hz, 6H, SiMe), 1.21 (d, $^2J_{PH}$ = 8.4 Hz, $^3J_{PtH}$ = 24.6 Hz, 9H, PMe), 1.54 (d, $^2J_{PH}$ = 8.1 Hz, $^3J_{PtH}$ = 16.8 Hz, 9H, PMe), 7.1−7.3 (m, 3H, Ph), 7.44−7.56 (m, 2H, Ph). $^{13}C\{^1H\}$ NMR (CD_2Cl_2, −50 °C): δ −2.7 (dd, $^3J_{PC}$ = 11 and 4 Hz, $^2J_{PtC}$ = 71 Hz, $^1J_{SnH}$ = 182 Hz, SnMe), 7.3 (dd, $^3J_{PC}$ = 7 and 4 Hz, $^2J_{PtC}$ = 75 Hz, SiMe), 18.5 (dd, $^1J_{PC}$ = 28 Hz, $^3J_{PC}$ = 6 Hz, $^2J_{PtC}$ = 23 Hz, PMe), 19.6 (dd, $^1J_{PC}$ = 24 Hz, $^3J_{PC}$ = 4 Hz, $^2J_{PtC}$ = 25 Hz, PMe), 126.5 (s, SiPh), 126.7 (s, SiPh), 134.5 (s, $^3J_{PtC}$ = 17 Hz, SiPh), 151.6 (t, $^3J_{PC}$ = 8 Hz, SiPh). $^{31}P\{^1H\}$ NMR (CD_2Cl_2, −50 °C): δ −15.1 (d, $^2J_{PP}$ = 27 Hz, $^1J_{PtP}$ = 1464 Hz, $^2J^{119}_{SnP}$ = 201 Hz, $^2J^{117}_{SnP}$ = 193 Hz), −17.8 (d, $^2J_{PP}$ = 27 Hz, $^1J_{PtP}$ = 2309 Hz, $^2J^{119}_{SnP}$ = 1645 Hz, $^2J^{117}_{SnP}$ = 1521 Hz). Anal. Calcd for $C_{17}H_{38}P_2SiSnPt$: C, 31.59; H, 5.93. Found: C, 31.20; H, 5.42.

Complex 1f. ^1H NMR (CD_2Cl_2, −50 °C): δ −0.04 (s, $^3J_{PtH}$ = 8.7 Hz, $^2J_{SnH}$ = 36.6 Hz, 9H, SnMe), 0.42 (s, $^3J_{PtH}$ = 22.8 Hz, 6H, SiMe), 0.80 (br, 9H, PCH_2CH_3), 1.01 (br, 9H, PCH_2CH_3), 1.77 (br, 6H, PCH_2CH_3), 1.90 (br, 6H, PCH_2CH_3), 7.1−7.2 (m, 3H, Ph), 7.42 (m, 2H, Ph). $^{13}C\{^1H\}$ NMR (CD_2Cl_2, −50 °C): δ −1.9 (t, $^3J_{PC}$ = 7 Hz, $^2J_{PtC}$ = 75 Hz, $^1J_{SnC}$ = 160 Hz, SnMe), 7.8 (dd, $^3J_{PC}$ = 6 and 5 Hz, $^2J_{PtC}$ = 73 Hz, SiMe), 8.7 (d, $^3J_{PC}$ = 9 Hz, PCH_2CH_3), 18.6 (br, PCH_2CH_3), 20.1 (br d, $^1J_{PC}$ = 18 Hz, PCH_2CH_3), 126.4 (s, SiPh), 126.8 (s, SiPh), 133.8 (s, $^3J_{PtC}$ = 14 Hz, SiPh), 152.1 (t, $^3J_{PC}$ = 8 Hz, $^2J_{PtC}$ = 31 Hz, SiPh). $^{31}P\{^1H\}$ NMR (CD_2Cl_2, −50 °C): δ 14.5 (br d, $^2J_{PP}$ = 23 Hz, $^1J_{PtP}$ = 1629 Hz, $^2J_{SnP}$ = 185 Hz), 13.6 (br d, $^2J_{PP}$ = 23 Hz, $^1J_{PtP}$ = 2513 Hz, $^2J_{SnP}$ = 1616 Hz). Anal. Calcd for $C_{23}H_{50}P_2SiSnPt$: C, 37.82; H, 6.90. Found: C, 37.54; H, 6.93.

Complex 1g. ^1H NMR (CD_2Cl_2, −50 °C): δ −0.27 (s, $^3J_{PtH}$ = 7.5 Hz, $^2J_{SnH}$ = 37.8 Hz, 9H, SnMe), 0.25 (s, $^3J_{PtH}$ = 22.8 Hz, 6H, SiMe), 1.31 (br, 3H, PMe), 1.50 (br, 3H, PMe), 7.2−7.8 (m, 25H, Ph). $^{13}C\{^1H\}$ NMR (CD_2Cl_2, −50 °C): δ −2.6 (t, $^3J_{PC}$ = 7 Hz, $^2J_{PtC}$ = 75 Hz, SnMe), 7.2 (t, $^3J_{PC}$ = 6 Hz, $^2J_{PtC}$ = 67 Hz, SiMe), 13.9 (br, PMe), 14.1 (br, PMe), 126.7 (s, SiPh), 127.8 (d, $^3J_{PC}$ = 8 Hz, PPh), 129.3 (s, PPh), 131.6 (d, $^2J_{PC}$ = 10 Hz, PPh), 134.6 (s, $^3J_{PtC}$ = 18 Hz, SiPh), 137.6 (br, PPh), 138.1 (br, PPh), 150.6 (t, $^3J_{PC}$ = 6 Hz, $^2J_{PtC}$ = 27 Hz, SiPh). $^{31}P\{^1H\}$

(11) Crascall, L. E.; Spencer, J. L. *Inorg. Synth.* **1990**, *28*, 126.

NMR (CD_2Cl_2, −50 °C): δ 9.3 (br d, $^2J_{PP}$ = 21 Hz, $^1J_{PtP}$ = 1596 Hz, $^2J_{SnP}$ = 197 Hz), 6.2 (br d, $^2J_{PP}$ = 21 Hz, $^1J_{PtP}$ = 2461 Hz, $^2J_{SnP}$ = 1540 Hz). Anal. Calcd for $C_{37}H_{46}P_2SiSnPt$: C, 49.68; H, 5.18. Found: C, 49.53; H, 5.20.

Reaction of 1d with Phenylacetylene. The time course of the reaction of **1d** with phenylacetylene shown in Figure 3 was followed by ^{1}H NMR spectroscopy. For example, **1d** (10.8 mg, 12.1 μmol) was placed in an NMR sample tube equipped with a rubber septum cap and dissolved in $CDCl_3$ (0.6 mL) at room temperature. Dimethylphenylphosphine (1.7 μL, 11.9 μmol) and phenylacetylene (13 μL, 0.12 mmol) were added, and the sample tube was placed in an NMR sample probe controlled at 50 °C. Relative amounts of **1d**, **2d**, and **3d** at time t were determined by peak integration of the $SnMe_3$ signals, which appeared at δ −0.31 (**1d**), 0.22 (**2d**), and −0.26 (**3d**), respectively, in the ^{1}H NMR spectrum at 50 °C.

Identification of *cis*-Pt{C(Ph)=CH(SnMe$_3$)}(SiPh$_3$)(PMe$_2$Ph)$_2$ (2d). Complex **3d** was independently prepared and identified by NMR spectroscopy and elemental analysis (vide infra). On the other hand, since **2d** is readily converted to **3d** in neat solvents, its formation was confirmed by NMR spectroscopy without isolation. The sample solution was prepared by the treatment of **1d** (20.5 mg, 22.9 μmol) with phenylacetylene (2.5 μL, 26.3 μmol) in CD_2Cl_2 (0.6 mL) in the presence of PMe_2Ph (3.2 μL, 22 μmol). Heating the sample at 35 °C for 1 day led to a solution containing a 93/7 ratio of **2d** and **3d**. The following NMR signals were observed for **2d**, clearly distinct from the peaks of free PMe_2Ph and **3d**. Thus, the vinylic proton signal appeared at δ 8.46 as a doublet of doublets (J_{PH} = 5.4 and 3.9 Hz) with the satellites arising from H−Sn couplings (224 Hz, the mean value of the $^2J_{^{119}SnH}$ and $^2J_{^{117}SnH}$). The observed coupling constants were consistent with the arrangement of atoms in the $(PhMe_2P)_2PtC(Ph)$=$CHSnMe_3$ moiety. On the other hand, in the $^{13}C\{^1H\}$ NMR spectrum, the α-vinylic carbon signal was observed at δ 169.4 as a doublet of doublets with platinum satellites ($^2J_{PC}$ = 99 and 17 Hz, $^1J_{PtC}$ = 713 Hz), which disappeared in a DEPT NMR spectrum because of the absence of a proton on this carbon. The $^{31}P\{^1H\}$ NMR signals did not involve P−Sn couplings, showing the absence of a Pt−Sn bond. The $^1J_{PtP}$ values were consistent with the alkenyl(silyl)platinum(II) structure.

Complex 2d. ^{1}H NMR (CD_2Cl_2, 20 °C): δ 0.19 (s, $^2J_{^{119}SnH}$ = 52.0 Hz, $^2J_{^{117}SnH}$ = 48.0 Hz, 9H, SnMe), 0.89 (d, $^2J_{PH}$ = 8.0 Hz, $^3J_{PtH}$ = 24.0 Hz, 3H, PMe), 1.20 (d, $^2J_{PH}$ = 8.0 Hz, $^3J_{PtH}$ = 16.0 Hz, 3H, PMe), 1.33 (d, $^2J_{PH}$ = 8.0 Hz, $^3J_{PtH}$ = 24.0 Hz, 3H, PMe), 1.42 (d, $^2J_{PH}$ = 8.0 Hz, $^3J_{PtH}$ = 16.0 Hz, 3H, PMe), 8.46 (dd, $^4J_{PH}$ = 5.4 and 3.9 Hz, $^3J_{PtH}$ = 14 Hz, $^2J_{SnH}$ = 224 Hz, 1H, PtC=C*H*). $^{13}C\{^1H\}$ NMR (CD_2Cl_2, 20 °C): δ −6.0 (s, $^1J_{^{119}SnC}$ = 414 Hz, $^1J_{^{117}SnC}$ = 304 Hz, SnMe), 12.0 (d, $^1J_{PC}$ = 21 Hz, PMe), 15.2 (d, $^1J_{PC}$ = 30 Hz, $^2J_{PtC}$ = 30 Hz, PMe), 16.7 (dd, $^1J_{PC}$ = 26 Hz, $^3J_{PC}$ = 5 Hz, $^2J_{PtC}$ = 26 Hz, PMe), 17.6 (dd, $^1J_{PC}$ = 29 Hz, $^3J_{PC}$ = 5 Hz, $^2J_{PtC}$ = 26 Hz, PMe), 137.1 (s, $^3J_{PtC}$ = 21 Hz, SiPh), 144.7 (d, $^3J_{PC}$ = 3 Hz, $^2J_{PtC}$ = 53 Hz, SiPh), 152.7 (dd, $^3J_{PC}$ = 14 and 4 Hz, Ph), 169.4 (dd, $^2J_{PC}$ = 99 and 17 Hz, $^1J_{PtC}$ = 713 Hz, Pt*C*=CH). $^{31}P\{^1H\}$ NMR (CD_2Cl_2, 20 °C): δ −10.9 (d, $^2J_{PP}$ = 19 Hz, $^1J_{PtP}$ = 1324 Hz), −15.5 (d, $^2J_{PP}$ = 19 Hz, $^1J_{PtP}$ = 1889 Hz).

Preparation of *cis*-Pt{C(Ph)=CH(SiPh$_3$)}(SnMe$_3$)(PMe$_2$Ph)$_2$ (3d). Analytically pure **3d** was obtained by the following procedure. Complex **1d** (150 mg, 0.168 mmol) was dissolved in CH_2Cl_2 (5 mL), and phenylacetylene (79.6 mg, 0.779 mmol) was added. The reddish yellow mixture was stirred at room temperature for 24 h to give a pale yellow solution, which was concentrated to almost dryness by pumping. Et_2O (1 mL) and pentane (3 mL) were added, and the resulting solid was collected by filtration, washed with pentane (1 mL × 3), and dried under vacuum. Recrystallization of the crude product from a mixture of CH_2Cl_2 and Et_2O gave white crystals of **3d** (102 mg, 61%).

Complex 3d. ^{1}H NMR (CD_2Cl_2, 20 °C): δ −0.32 (s, $^3J_{PtH}$ = 4.2 Hz, $^2J_{SnH}$ = 37.5 Hz, 9H, SnMe), 0.83 (d, $^2J_{PH}$ = 8.4 Hz, $^3J_{PtH}$ = 30.0 Hz, 3H, PMe), 1.02 (d, $^2J_{PH}$ = 8.7 Hz, $^3J_{PtH}$ = 32.3 Hz, 3H, PMe), 1.20 (d, $^2J_{PH}$ = 7.8 Hz, $^3J_{PtH}$ = 28.2 Hz, 3H, PMe), 1.65 (d, $^2J_{PH}$ = 8.1 Hz, $^3J_{PtH}$ = 35.7 Hz, 3H, PMe), 6.67 (t, 2H, Ph), 7.04 (t, 2H, Ph), 7.1−7.4 (m, 17H, Ph), 7.67 (d, 6H, Ph), 7.84 (d, 2H, Ph), 8.08 (dd, $^4J_{PH}$ = 19.5 and 4.2 Hz, $^3J_{PtH}$ = 96.9 Hz, 1H, PtC=C*H*). $^{13}C\{^1H\}$ NMR (CD_2Cl_2, 20 °C): δ −3.8 (d, $^3J_{PC}$ = 10 Hz, $^2J_{PtC}$ = 74 Hz, $^1J_{SnC}$ = 183 Hz, SnMe), 12.8 (d, $^1J_{PC}$ = 26 Hz, $^2J_{PtC}$ = 26 Hz, PMe), 14.5 (dd, $^1J_{PC}$ = 30 Hz, $^3J_{PC}$ = 3 Hz, $^2J_{PtH}$ = 36 Hz, PMe), 18.4 (dd, $^1J_{PC}$ = 30 Hz, $^3J_{PC}$ = 7 Hz, $^3J_{PtH}$ = 17 Hz, PMe), 20.1 (dd, $^1J_{PC}$ = 33 Hz, $^3J_{PC}$ = 5 Hz, $^3J_{PtH}$ = 50 Hz, PMe), 125.8 (t, $^3J_{PC}$ = 6 Hz, $^2J_{PtC}$ = 56 Hz, PtC=*C*H), 126.6 (s, $^5J_{PtC}$ = 4 Hz, Ph), 127.8 (s, SiPh), 127.8 (s, Ph), 128.3 (d, $^3J_{PC}$ = 8 Hz, PPh), 128.3 (d, $^3J_{PC}$ = 10 Hz, PPh), 129.2 (s, SiPh), 129.4 (s, Ph), 129.7 (s, PPh), 129.9 (s, PPh), 130.5 (d, $^2J_{PC}$ = 10 Hz, $^3J_{PtC}$ = 10 Hz, PPh), 131.5 (d, $^2J_{PC}$ = 10 Hz, $^3J_{PtC}$ = 20 Hz, PPh), 137.1 (s, SiPh), 138.4 (s, SiPh), 154.1 (d, $^3J_{PC}$ = 3 Hz, $^2J_{PtC}$ = 33 Hz, Ph), 184.3 (dd, $^2J_{PC}$ = 101 and 13 Hz, $^1J_{PtH}$ = 719 Hz, Pt*C*=CH). The two ipso carbon signals of PPh groups at δ 138−139 were obscured. $^{31}P\{^1H\}$ NMR (CD_2Cl_2, 20 °C): δ −15.3 (d, $^2J_{PP}$ = 18 Hz, $^1J_{PtP}$ = 2081 Hz, $^2J_{^{119}SnP}$ = 1736 Hz, $^2J_{^{117}SnP}$ = 1659 Hz), −18.6 (d, $^2J_{PP}$ = 18 Hz, $^1J_{PtP}$ = 1975 Hz, $^2J_{^{119}SnP}$ = 171 Hz, $^2J_{^{117}SnP}$ = 164 Hz). Anal. Calcd for $C_{45}H_{52}P_2SiSnPt$: C, 54.23; H, 5.26. Found: C, 53.95; H, 5.19.

Identification of 2. Complexes **2b**, **2c**, and **2e**−**j** were prepared similarly to **2d** and characterized by NMR spectroscopy without isolation. The $^{31}P\{^1H\}$ NMR spectra exhibited two sets of doublets with small (1181−1302 Hz) and moderate (1825−2000 Hz) couplings to platinum, respectively. These $^1J_{PtP}$ values were consistent with the structures having alkenyl and silyl ligands in mutually cis positions, as already seen for **2d**. Since the selectivities for these complexes were much lower than that for **2d**, a rather limited number of ^{1}H NMR signals were assignable, while the β-vinylic proton signals were clearly detected at a significantly lower magnetic field (δ 8.25−9.07) with $^4J_{PH}$ values (4−5 Hz) comparable to **2d**.

Complex 2b. ^{1}H NMR (CD_2Cl_2, −5 °C): δ 0.23 (s, 6H, SiMe), 0.24 (s, 9H, SnMe), 8.68 (dd, $^4J_{PH}$ = 4.5 and 4.2 Hz, 1H, PtC=C*H*). $^{31}P\{^1H\}$ NMR (CD_2Cl_2, −5 °C): δ −11.7 (d, $^2J_{PP}$ = 18 Hz, $^1J_{PtP}$ = 1193 Hz), −15.3 (d, $^2J_{PP}$ = 18 Hz, $^1J_{PtP}$ = 1868 Hz).

Complex 2c. ^{1}H NMR (CD_2Cl_2, −5 °C): δ 0.30 (s, 9H, SnMe), 0.31 (s, 3H, SiMe), 8.51 (dd, $^4J_{PH}$ = 5.4 and 3.9 Hz, $^3J_{PtH}$ = 14 Hz, $^2J_{SnH}$ = 213 Hz, 1H, PtC=C*H*). $^{31}P\{^1H\}$ NMR (CD_2Cl_2, −5 °C): δ −9.1 (d, $^2J_{PP}$ = 18 Hz, $^1J_{PtP}$ = 1302 Hz), −14.2 (d, $^2J_{PP}$ = 18 Hz, $^1J_{PtP}$ = 1966 Hz).

Complex 2e. ^{1}H NMR (CD_2Cl_2, −5 °C): δ 0.23 (s, 9H, SnMe), 0.24 (s, 6H, SiMe), 8.73 (t, $^4J_{PH}$ = 4.8 Hz, 1H, PtC=C*H*). $^{31}P\{^1H\}$ NMR (CD_2Cl_2, −5 °C): δ −21.4 (d, $^2J_{PP}$ = 18 Hz, $^1J_{PtP}$ = 1206 Hz), −28.2 (d, $^2J_{PP}$ = 18 Hz, $^1J_{PtP}$ = 1825 Hz).

Complex 2f. ^{1}H NMR (CD_2Cl_2, −5 °C): δ 0.25 (s, 6H, SiMe), 0.27 (s, 9H, SnMe), 8.49 (t, $^4J_{PH}$ = 4.5 Hz, 1H, PtC=C*H*). $^{31}P\{^1H\}$ NMR (CD_2Cl_2, −5 °C): δ −0.6 (d, $^2J_{PP}$ = 20 Hz, $^1J_{PtP}$ = 1201 Hz), 0.1 (d, $^2J_{PP}$ = 20 Hz, $^1J_{PtP}$ = 1875 Hz).

Complex 2g. ^{1}H NMR (CD_2Cl_2, −5 °C): δ 0.33 (s, 6H, SiMe), 0.40 (s, 9H, SnMe), 8.25 (t, $^4J_{PH}$ = 4.8 Hz, 1H, PtC=C*H*). $^{31}P\{^1H\}$ NMR (CD_2Cl_2, −5 °C): δ 4.0 (d, $^2J_{PP}$ = 16 Hz, $^1J_{PtP}$ = 1190 Hz), −0.6 (d, $^2J_{PP}$ = 16 Hz, $^1J_{PtP}$ = 1891 Hz).

Complex 2h. ^{1}H NMR (CD_2Cl_2, −5 °C): δ 0.30 (s, 6H, SiMe), 0.32 (s, 9H, SnMe), 3.49 (s, 2H, NH_2), 8.53 (t, $^4J_{PH}$ = 4.5 Hz, 1H, PtC=C*H*). $^{31}P\{^1H\}$ NMR (CD_2Cl_2, −5 °C): δ −11.4 (d, $^2J_{PP}$ = 17 Hz, $^1J_{PtP}$ = 1191 Hz), −15.6 (d, $^2J_{PP}$ = 17 Hz, $^1J_{PtP}$ = 1846 Hz).

Complex 2i. ^{1}H NMR (CD_2Cl_2, −5 °C): δ 0.31 (s, 6H, SiMe), 0.33 (s, 9H, SnMe), 2.25 (s, 3H, *p*-Me), 8.78 (t, $^4J_{PH}$ = 5.1 Hz, 1H, PtC=C*H*). $^{31}P\{^1H\}$ NMR (CD_2Cl_2, −5 °C): δ −11.7 (d, $^2J_{PP}$ = 18 Hz, $^1J_{PtP}$ = 1181 Hz), −15.6 (d, $^2J_{PP}$ = 18 Hz, $^1J_{PtP}$ = 1858 Hz).

Complex 2j. ^{1}H NMR (CD_2Cl_2, −5 °C): δ 0.33 (s, 6H, SiMe), 0.37 (s, 9H, SnMe), 9.07 (t, $^4J_{PH}$ = 3.9 Hz, 1H, PtC=C*H*), 10.0

(s, 1H, CHO). $^{31}P\{^1H\}$ NMR (CD_2Cl_2, −5 °C): δ −9.3 (d, $^2J_{PP}$ = 20 Hz, $^1J_{PtP}$ = 1224 Hz), −15.6 (d, $^2J_{PP}$ = 20 Hz, $^1J_{PtP}$ = 2000 Hz).

Preparation of *cis*-Pt{C(CO$_2$Me)=C(CO$_2$Me)(SnMe$_3$)}-(SiMe$_2$Ph)(PMe$_2$Ph)$_2$ (2k). To a solution of **1b** (80 mg, 0.10 mmol) in CH_2Cl_2 (5 mL) was added dimethyl acetylenedicarboxylate (30 mg, 0.21 mmol) at −50 °C. The initially pale yellow color of the solution instantly changed to red. The solvent was removed by pumping at 0 °C. The resulting oily material was cooled to −78 °C and dissolved in Et_2O (0.5 mL). Addition of pentane (1 mL) with stirring led to precipitation of a reddish orange powder, which was collected by filtration, washed with pentane (1 mL × 2), and dried under vacuum (73 mg, 77%). Analytically pure compound was obtained by recrystallization from CH_2Cl_2 and Et_2O.

Complex 2k. ^1H NMR (CD_2Cl_2, 20 °C): δ 0.54 (s, $^2J_{^{119}SnP}$ = 54.0 Hz, $^2J_{^{117}SnH}$ = 51.6 Hz, 9H, SnMe), 0.56 (d, $^4J_{PH}$ = 2.4 Hz, $^3J_{PtH}$ = 19.8 Hz, 6H, SiMe), 1.07 (d, $^2J_{PH}$ = 8.7 Hz, $^3J_{PtH}$ = 26.4 Hz, 3H, PMe), 1.17 (d, $^2J_{PH}$ = 8.4 Hz, $^3J_{PtH}$ = 23.4 Hz, 3H, PMe), 1.43 (d, $^2J_{PH}$ = 8.4 Hz, $^3J_{PtH}$ = 15.6 Hz, 3H, PMe), 1.50 (d, $^2J_{PH}$ = 8.4 Hz, $^3J_{PtH}$ = 15.6 Hz, 3H, PMe), 3.70 (s, 6H, CO_2Me), 7.1−7.9 (m, 20H, Ph). $^{13}C\{^1H\}$ NMR (CD_2Cl_2, 20 °C): δ −6.0 (s, $^1J_{^{119}SnC}$ = 351 Hz, $^1J_{^{117}SnC}$ = 336 Hz, SnMe), 5.7 (d, $^3J_{PC}$ = 7 Hz, $^2J_{PtC}$ = 53 Hz, SiMe), 12.8 (d, $^1J_{PC}$ = 25 Hz, $^2J_{PtC}$ = 26 Hz, PMe), 15.1 (dd, $^1J_{PC}$ = 32 Hz, $^3J_{PC}$ = 3 Hz, $^2J_{PtC}$ = 25 Hz, PMe), 15.6 (dd, $^1J_{PC}$ = 27 Hz, $^3J_{PC}$ = 2 Hz,$^2J_{PtC}$ = 24 Hz, PMe), 18.2 (dd, $^1J_{PC}$ = 28 Hz, $^3J_{PC}$ = 6 Hz, $^2J_{PtC}$ = 45 Hz, PMe), 50.6 (s, CO_2*Me*), 51.3 (s, CO_2*Me*), 127.3 (s, SiPh), 128.4 (d, $^3J_{PC}$ = 9 Hz, PPh), 128.5 (d, $^3J_{PC}$ = 9 Hz, PPh), 129.8 (d, $^4J_{PC}$ = 2 Hz, PPh), 130.0 (d, $^4J_{PC}$ = 2 Hz, PPh), 130.8 (d, $^2J_{PC}$ = 11 Hz, $^3J_{PtP}$ = 14 Hz, PPh), 131.2 (d, $^2J_{PC}$ = 11 Hz, $^3J_{PtP}$ = 7 Hz, PPh), 132.5 (t, $^3J_{PC}$ = 13 Hz, $^2J_{PtC}$ = 27 Hz, PtC=*C*), 134.7 (s, $^3J_{PtC}$ = 9 Hz, SiPh), 137.8 (dd, $^1J_{PC}$ = 44 Hz, $^3J_{PC}$ = 5 Hz, PPh), 137.9 (dd, $^1J_{PC}$ = 39 Hz, $^3J_{PC}$ = 5 Hz, PPh), 150.6 (dd, $^3J_{PC}$ = 7 and 3 Hz, $^2J_{PtC}$ = 45 Hz, SiPh), 168.8 (dd, $^3J_{PC}$ = 14 and 4 Hz, PtC(*C*O$_2$Me)=C), 177.3 (d, $^4J_{PC}$ = 3 Hz, PtC=C(*C*O$_2$Me)), 193.9 (dd, $^2J_{PC}$ = 98 and 15 Hz, Pt*C*=C). $^{31}P\{^1H\}$ NMR (CD_2Cl_2, 20 °C): δ −10.9 (d, $^2J_{PP}$ = 21 Hz, $^1J_{PtP}$ = 1203 Hz), −16.4 (d, $^2J_{PP}$ = 21 Hz, $^1J_{PtP}$ = 2168 Hz). Anal. Calcd for $C_{33}H_{48}O_4P_2SiSnPt$: C, 43.43; H, 5.30. Found: C, 43.41; H, 5.31.

Preparation of 3. The complexes resulting from alkyne insertion into the Pt−Si bond of **1** were prepared similarly to **3d** in 60% (**3a**), 67% (**3b**), 52% (**3c**), 82% (**3e**), 76% (**3f**), 48% (**3g**), 62% (**3h**), 72% (**3i**), and 55% (**3j**) yields, respectively.

Complex 3a. ^1H NMR (CD_2Cl_2, 20 °C): δ −0.12 (s, $^3J_{PtH}$ = 7.5 Hz, $^2J_{SnH}$ = 37.5 Hz, 9H, SnMe), 0.28 (s, 9H, SiMe), 1.14 (d, $^2J_{PH}$ = 8.4 Hz, $^3J_{PtH}$ = 25.2 Hz, 3H, PMe), 1.35 (d, $^3J_{PH}$ = 8.1 Hz, $^2J_{PtH}$ = 22.8 Hz, 3H, PMe), 1.47 (d, $^3J_{PH}$ = 8.1 Hz, $^2J_{PtH}$ = 22.8 Hz, 3H, PMe), 1.59 (d, $^3J_{PH}$ = 8.1 Hz, $^2J_{PtH}$ = 25.2 Hz, 3H, PMe), 7.0−7.6 (m, 14H, Ph and PtC=C*H*), 7.72 (m, 2H, Ph). $^{13}C\{^1H\}$ NMR (CD_2Cl_2, 20 °C): δ −4.2 (dd, $^3J_{PC}$ = 10 and 2 Hz, $^2J_{PtC}$ = 77 Hz, $^1J_{SnC}$ = 186 Hz, SnMe), 1.0 (s, SiMe), 13.6 (dd, $^1J_{PC}$ = 26 Hz, $^3J_{PC}$ = 2 Hz, $^2J_{PtC}$ = 29 Hz, PMe), 14.5 (dd, $^1J_{PC}$ = 29 Hz, $^3J_{PC}$ = 3 Hz, $^2J_{PtC}$ = 39 Hz, PMe), 18.7 (dd, $^1J_{PC}$ = 30 Hz, $^3J_{PC}$ = 5 Hz, $^2J_{PtC}$ = 30 Hz, PMe), 19.2 (dd, $^1J_{PC}$ = 31 Hz, $^3J_{PC}$= 5 Hz, $^2J_{PtC}$ = 40 Hz, PMe), 125.9 (s, $^5J_{PtC}$ = 6 Hz, Ph), 127.6 (s, Ph), 128.5 (d, $^3J_{PC}$ = 9 Hz, PPh), 129.2 (d, $^4J_{PC}$ = 2 Hz, $^3J_{PtC}$ = 46 Hz, Ph), 129.7 (s, PPh), 130.8 (d, $^2J_{PC}$ = 12 Hz, PPh), 130.9 (d, $^2J_{PC}$ = 11 Hz, PPh), 131.5 (t, $^3J_{PC}$ = 7 Hz, $^2J_{PtC}$ = 43 Hz, PtC=*C*H), 138.1 (dd, $^1J_{PC}$ = 36 Hz, $^3J_{PC}$ = 2 Hz, $^2J_{PtC}$ = 21 Hz, PPh), 139.0 (dd, $^1J_{PC}$ = 42 Hz, $^3J_{PC}$ = 3 Hz, $^2J_{PtC}$ = 17 Hz, PPh), 153.6 (dd, $^3J_{PC}$ = 5 and 2 Hz, $^2J_{PtC}$ = 30 Hz, Ph), 175.9 (dd, $^2J_{PC}$ = 97 and 14 Hz, $^1J_{PtC}$ = 703 Hz, Pt*C*=CH). $^{31}P\{^1H\}$ NMR (CD_2Cl_2, 20 °C): δ −14.1 (d, $^2J_{PP}$ = 17 Hz, $^1J_{PtP}$ = 2081 Hz, $^2J_{^{119}SnP}$ = 1784 Hz, $^2J_{^{117}SnP}$ = 1704 Hz), −16.3 (d, $^2J_{PP}$ = 17 Hz, $^1J_{PtP}$ = 1927 Hz, $^2J_{^{119}SnP}$ = 168 Hz, $^2J_{^{117}SnP}$ = 161 Hz). Anal. Calcd for $C_{30}H_{46}P_2SiSnPt$: C, 44.46; H, 5.72. Found: C, 44.43; H, 5.71.

Complex 3b. ^1H NMR (CD_2Cl_2, 20 °C): δ −0.11 (s, $^3J_{PtH}$ = 7.5 Hz, $^2J_{SnH}$ = 37.5 Hz, 9H, SnMe), 0.51 (s, 3H, SiMe), 0.71 (s, 3H, SiMe), 1.04 (d, $^2J_{PH}$ = 8.7 Hz, $^3J_{PtH}$ = 33.6 Hz, 3H, PMe), 1.15 (d, $^2J_{PH}$ = 8.1 Hz, $^3J_{PtH}$ = 31.2 Hz, 3H, PMe), 1.48 (d, $^2J_{PH}$ = 7.8 Hz, $^3J_{PtH}$ = 25.8 Hz, 3H, PMe), 1.58 (d, $^2J_{PH}$ = 7.8 Hz, $^3J_{PtH}$ = 27.6 Hz, 3H, PMe), 7.0−7.4 (m, 16H, Ph), 7.51 (dd, $^4J_{PH}$ = 19.8 and 4.5 Hz, 1H, PtC=C*H*), 7.67 (m, 2H, Ph), 7.77 (m, 2H, Ph). $^{13}C\{^1H\}$ NMR (CD_2Cl_2, 20 °C): δ −4.1 (dd, $^3J_{PC}$ = 10 and 2 Hz, $^2J_{PtC}$ = 78 Hz, $^1J_{SnC}$ = 191 Hz, SnMe), 0.20 (s, SiMe), 13.4 (dd, $^1J_{PC}$ = 26 Hz, $^3J_{PC}$ = 2 Hz, $^2J_{PtC}$ = 27 Hz, PMe), 14.5 (dd, $^1J_{PC}$ = 29 Hz, $^3J_{PC}$ = 3 Hz, $^2J_{PtC}$ = 39 Hz, PMe), 18.8 (dd, $^1J_{PC}$ = 17 Hz, $^3J_{PC}$ = 5 Hz, PMe), 19.2 (dd, $^1J_{PC}$ = 18 Hz, $^3J_{PH}$ = 5 Hz, PMe), 126.2 (s, $^5J_{PtC}$ = 6 Hz, Ph), 127.7 (s, Ph), 127.9 (s, SiPh), 128.4 (d, $^3J_{PC}$ = 9 Hz, PPh), 128.5 (s, SiPh), 128.5 (d, $^3J_{PC}$ = 9 Hz, PPh), 129.4 (d, $^4J_{PC}$ = 2 Hz, $^3J_{PtC}$ = 45 Hz, Ph), 129.7 (d, $^4J_{PC}$ = 2 Hz, PPh), 129.8 (d, $^4J_{PC}$ = 2 Hz, PPh), 130.8 (d, $^2J_{PC}$ = 12 Hz, $^3J_{PtC}$ = 14 Hz, PPh), 130.9 (d, $^2J_{PC}$ = 12 Hz, $^3J_{PtC}$ = 15 Hz, PPh), 134.4 (s, SiPh), 138.1 (dd, $^1J_{PC}$ = 36 Hz, $^3J_{PC}$ = 2 Hz, $^2J_{PtC}$ = 17 Hz, PPh), 138.9 (dd, $^1J_{PC}$ = 42 Hz, $^3J_{PC}$ = 4 Hz, $^2J_{PtC}$ = 15 Hz, PPh), 142.9 (s, SiPh), 153.4 (dd, $^3J_{PC}$ = 5 and 2 Hz, $^2J_{PtC}$ = 37 Hz, Ph), 178.8 (dd, $^2J_{PC}$ = 100 and 14 Hz, Pt*C*=CH). The β-vinylic carbon signal was not assigned. $^{31}P\{^1H\}$ NMR (CD_2Cl_2, 20 °C): δ −14.0 (d, $^2J_{PP}$ = 17 Hz, $^1J_{PtP}$ = 2071 Hz, $^2J_{^{119}SnP}$ = 1771 Hz, $^2J_{^{117}SnP}$ = 1692 Hz), −16.7 (d, $^2J_{PP}$ = 18 Hz, $^1J_{PtP}$ = 1928 Hz, $^2J_{^{119}SnP}$ = 166 Hz, $^2J_{^{117}SnP}$ = 159 Hz). Anal. Calcd for $C_{35}H_{48}P_2SiSnPt$: C, 48.18; H, 5.54. Found: C, 47.93; H, 5.44.

Complex 3c. ^1H NMR (CD_2Cl_2, 20 °C): δ −0.20 (s, $^3J_{PtH}$ = 7.5 Hz, $^2J_{SnH}$ = 37.8 Hz, 9H, SnMe), 1.03 (s, 3H, SiMe), 0.78 (d, $^2J_{PH}$ = 8.4 Hz, $^3J_{PtH}$ = 33.6 Hz, 3H, PMe), 0.86 (d, $^2J_{PH}$ = 8.7 Hz, $^3J_{PtH}$ = 33.6 Hz, 3H, PMe), 1.40 (d, $^2J_{PH}$ = 8.1 Hz, $^3J_{PtH}$ = 31.2 Hz, 3H, PMe), 1.44 (d, $^2J_{PH}$ = 7.8 Hz, $^3J_{PtH}$ = 25.8 Hz, 3H, PMe), 1.44 (d, $^2J_{PH}$ = 7.8 Hz, $^3J_{PtH}$ = 27.6 Hz, 3H, PMe), 6.8−7.8 (m, 25H, Ph), 7.96 (dd, $^4J_{PH}$ = 19.2 and 4.5 Hz, 1H, PtC=C*H*). $^{13}C\{^1H\}$ NMR (CD_2Cl_2, 20 °C): δ −4.2 (d, $^3J_{PC}$ = 10 Hz, $^2J_{PtC}$ = 77 Hz, $^1J_{SnC}$ = 193 Hz, SnMe), −1.5 (s, SiMe), 12.9 (d, $^1J_{PC}$ = 25 Hz, $^2J_{PtC}$ = 27 Hz, PMe), 14.6 (dd, $^1J_{PC}$ = 30 Hz, $^3J_{PC}$ = 3 Hz, $^2J_{PtC}$ = 41 Hz, PMe), 18.8 (dd, $^1J_{PC}$ = 31 Hz, $^3J_{PC}$ = 4 Hz, PMe), 19.0 (dd, $^1J_{PC}$ = 31 Hz, $^3J_{PC}$ = 6 Hz, PMe), 125.0 (t, $^3J_{PC}$ = 6 Hz, $^2J_{PtC}$ = 55 Hz, PtC=*C*H), 126.5 (s, $^5J_{PtC}$ = 4 Hz, Ph), 127.7 (s, Ph), 127.8 (s, SiPh), 128.0 (s, SiPh), 128.4 (d, $^3J_{PC}$ = 8 Hz, PPh), 128.5 (d, $^3J_{PC}$ = 9 Hz, PPh), 128.7 (s, SiPh), 128.9 (s, SiPh), 129.5 (d, $^4J_{PC}$ = 2 Hz, $^3J_{PtC}$ = 48 Hz, Ph), 129.7 (s, PPh), 129.9 (s, PPh), 130.7 (d, $^2J_{PC}$ = 11 Hz, $^3J_{PtC}$ = 15 Hz, PPh), 130.9 (d, $^2J_{PC}$ = 12 Hz, $^3J_{PtC}$ = 15 Hz, PPh), 135.1 (s, SiPh), 135.1 (s, SiPh), 138.1 (d, $^1J_{PC}$ = 37 Hz, $^2J_{PtC}$ = 17 Hz, PPh), 138.8 (dd, $^1J_{PC}$ = 43 and 3 Hz, $^2J_{PtC}$ = 14 Hz, PPh), 141.1 (s, SiPh), 141.2 (s, SiPh), 153.3 (dd, $^3J_{PC}$ = 5 and 1 Hz, $^2J_{PtC}$ = 35 Hz, Ph), 181.7 (dd, $^2J_{PC}$ = 100 and 13 Hz, $^1J_{PtC}$ = 712 Hz, Pt*C*=CH). $^{31}P\{^1H\}$ NMR (CD_2Cl_2, 20 °C): δ −13.8 (d, $^2J_{PP}$ = 18 Hz, $^1J_{PtP}$ = 2065 Hz, $^2J_{^{119}SnP}$ = 1742 Hz, $^2J_{^{117}SnP}$ = 1662 Hz), −16.7 (d, $^2J_{PP}$ = 18 Hz, $^1J_{PtP}$ = 1928 Hz, $^2J_{^{119}SnP}$ = 166 Hz, $^2J_{^{117}SnP}$ = 159 Hz). Anal. Calcd for $C_{40}H_{50}P_2SiSnPt$: C, 51.40; H, 5.39. Found: C, 51.32; H, 5.33.

Complex 3e. ^1H NMR (CD_2Cl_2, 20 °C): δ −0.11 (s, $^3J_{PtH}$ = 7.3 Hz, $^2J_{SnH}$ = 37.2 Hz, 9H, SnMe), 0.40 (s, 3H, SiMe), 0.55 (s, 3H, SiMe), 1.14 (d, $^2J_{PH}$ = 8.4 Hz, $^3J_{PtH}$ = 23.4 Hz, 9H, PMe), 1.62 (d, $^2J_{PH}$ = 8.1 Hz, $^3J_{PtH}$ = 23.1 Hz, 9H, PMe), 6.9−7.8 (m, 10H, Ph), 7.45 (dd, $^4J_{PH}$ = 19.8 and 4.2 Hz, 1H, PtC=C*H*). $^{13}C\{^1H\}$ NMR (CD_2Cl_2, 20 °C): δ −4.4 (dd, $^3J_{PC}$ = 10 and 2 Hz, $^2J_{PtC}$ = 77 Hz, SnMe), 0.1 (s, SiMe), 16.5 (dd, $^1J_{PC}$ = 26 Hz, $^3J_{PC}$ = 3 Hz, $^2J_{PtC}$ = 31 Hz, PMe), 20.6 (dd, $^1J_{PC}$ = 30 Hz, $^3J_{PH}$ = 5 Hz, $^2J_{PtC}$ = 33 Hz, PMe), 126.1 (s, $^5J_{PtC}$ = 5 Hz, Ph), 126.9 (t, $^3J_{PC}$ = 6 Hz, $^2J_{PtC}$ = 53 Hz, PtC=*C*H), 127.5 (s, Ph), 127.8 (s, SiPh), 128.4 (s, SiPh), 129.1 (d, $^4J_{PC}$ = 2 Hz, $^3J_{PtC}$ = 45 Hz, Ph), 134.3 (s, SiPh), 142.9 (s, SiPh), 153.0 (dd, $^3J_{PC}$ = 5 and 1 Hz, $^2J_{PtC}$ = 33 Hz, Ph), 179.1 (dd, $^2J_{PC}$ = 101 and 13 Hz, $^1J_{PtC}$ = 719 Hz, Pt*C*=CH). $^{31}P\{^1H\}$ NMR (CD_2Cl_2, 20 °C): δ −24.5 (d, $^2J_{PP}$ = 16 Hz, $^1J_{PtP}$ = 2078 Hz, $^2J_{^{119}SnP}$ = 1813 Hz, $^2J_{^{117}SnP}$ = 1731 Hz), −29.1 (d, $^2J_{PP}$ = 18 Hz, $^1J_{PtP}$ = 1878 Hz, $^2J_{^{119}SnP}$ = 172 Hz, $^2J_{^{117}SnP}$ = 164 Hz). Anal. Calcd for $C_{25}H_{44}P_2SiSnPt$: C, 40.12; H, 5.93. Found: C, 39.71; H, 5.63.

Complex 3f. ^1H NMR (CD_2Cl_2, 20 °C): δ 0.00 (s, $^3J_{PtH}$ = 6.3 Hz, $^2J_{SnH}$ = 35.4 Hz, 9H, SnMe), 0.43 (s, 3H, SiMe), 0.67

(s, 3H, SiMe), 0.68 (dt, $^3J_{PH}$ = 15.3 Hz, $^3J_{HH}$ = 7.5 Hz, 9H, PCH_2CH_3), 1.13 (dt, $^3J_{PH}$ = 15.3 Hz, $^3J_{HH}$ = 7.5 Hz, 9H, PCH_2CH_3), 1.57 (m, 6H, PCH_2CH_3), 1.97 (m, 6H, PCH_2CH_3), 7.05−7.60 (m, 6H, Ph), 7.45 (dd, $^4J_{PH}$ = 19.2 and 3.9 Hz, 1H, PtC=C*H*), 7.64−7.67 (m, 4H, Ph). $^{13}C\{^1H\}$ NMR (CD_2Cl_2, 20 °C): δ −2.9 (d, $^3J_{PC}$ = 10 Hz, $^2J_{PtC}$ = 74 Hz, $^1J_{SnC}$ = 189 Hz, SnMe), 0.5 (s, SiMe), 8.0 (d, $^2J_{PC}$ = 2 Hz, $^3J_{PtC}$ = 18 Hz, PCH_2CH_3), 8.6 (s, $^3J_{PtC}$ = 16 Hz, PCH_2CH_3), 16.7 (dd, $^1J_{PC}$ = 24 Hz, $^3J_{PC}$ = 2 Hz, $^2J_{PtC}$ = 28 Hz, PCH_2CH_3), 19.4 (dd, $^1J_{PC}$ = 27 Hz, $^3J_{PC}$ = 4 Hz, $^2J_{PtC}$ = 29 Hz, PCH_2CH_3), 125.8 (s, $^5J_{PtC}$ = 6 Hz, Ph), 127.4 (s, Ph), 127.7 (s, SiPh), 128.3 (s, SiPh), 129.2 (d, $^4J_{PC}$ = 2 Hz, $^3J_{PtC}$ = 44 Hz, Ph), 130.0 (t, $^3J_{PC}$ = 6 Hz, $^2J_{PtC}$ = 55 Hz, PtC=*C*H), 134.3 (s, SiPh), 143.1 (s, SiPh), 154.5 (dd, $^3J_{PC}$ = 5 and 2 Hz, $^2J_{PtC}$ = 33 Hz, Ph), 179.1 (dd, $^2J_{PC}$ = 98 and 13 Hz, $^1J_{PtC}$ = 698 Hz, Pt*C*=CH). $^{31}P\{^1H\}$ NMR (CD_2Cl_2, 20 °C): δ 2.9 (d, $^2J_{PP}$ = 16 Hz, $^1J_{PtP}$ = 1932 Hz, $^2J_{^{119}SnP}$ = 164 Hz, $^2J_{^{117}SnP}$ = 156 Hz), 0.1 (d, $^2J_{PP}$ = 18 Hz, $^1J_{PtP}$ = 2^{117} Hz, $^2J_{^{119}SnP}$ = 1770 Hz, $^2J_{^{117}SnP}$ = 1692 Hz). Anal. Calcd for $C_{31}H_{56}P_2SiSnPt$: C, 44.72; H, 6.78. Found: C, 44.74; H, 6.78.

Complex 3g. ^1H NMR (CD_2Cl_2, 20 °C): δ −0.18 (s, $^2J_{SnH}$ = 38.4 Hz, 9H, SnMe), 0.65 (s, 3H, SiMe), 0.90 (s, 3H, SiMe), 1.45 (d, $^2J_{PH}$ = 8.1 Hz, $^3J_{PtH}$ = 22.8 Hz, 3H, PMe), 2.05 (d, $^2J_{PH}$ = 7.5 Hz, $^3J_{PtH}$ = 24.6 Hz, 3H, PMe), 6.7−7.9 (m, 31H, Ph and PtC=C*H*). $^{13}C\{^1H\}$ NMR (CD_2Cl_2, 20 °C): δ −3.6 (dd, $^3J_{PC}$ = 10 and 2 Hz, $^2J_{PtC}$ = 76 Hz, $^1J_{SnC}$ = 194 Hz, SnMe), 0.1 (s, SiMe), 13.4 (dd, $^1J_{PC}$ = 28 Hz, $^3J_{PC}$ = 2 Hz, $^2J_{PtC}$ = 32 Hz, PMe), 19.7 (dd, $^1J_{PC}$ = 32 Hz, $^3J_{PH}$ = 5 Hz, $^2J_{PtC}$ = 36 Hz, PMe), 125.9 (s, $^5J_{PtC}$ = 6 Hz, Ph), 127.2 (s, Ph), 127.9 (s, SiPh), 128.4 (s, SiPh), 128.4 (m, PPh), 129.0 (d, $^4J_{PC}$ = 2 Hz, Ph), 129.3 (d, $^4J_{PC}$ = 2 Hz, PPh), 129.6 (d, $^4J_{PC}$ = 2 Hz, PPh), 130.2 (d, $^4J_{PC}$ = 2 Hz, PPh), 130.2 (d, $^4J_{PC}$ = 2 Hz, PPh), 132.2 (d, $^2J_{PC}$ = 10 Hz, $^3J_{PtC}$ = 14 Hz, PPh), 132.4 (d, $^2J_{PC}$ = 11 Hz, $^3J_{PtC}$ = 17 Hz, PPh), 133.2 (d, $^2J_{PC}$ = 12 Hz, $^3J_{PtC}$ = 15 Hz, PPh), 133.6 (d, $^2J_{PC}$ = 12 Hz, $^3J_{PtC}$ = 20 Hz, PPh), 134.3 (s, SiPh), 136.9 (dd, $^1J_{PC}$ = 45 Hz, $^3J_{PC}$ = 3 Hz, $^2J_{PtC}$ = 26 Hz, PPh), 137.9 (dd, $^1J_{PC}$ = 42 Hz, $^3J_{PC}$ = 5 Hz, $^2J_{PtC}$ = 26 Hz, PPh), 142.8 (s, SiPh), 153.0 (dd, $^3J_{PC}$ = 5 and 2 Hz, $^2J_{PtC}$ = 31 Hz, Ph), 177.5 (dd, $^2J_{PC}$ = 98 and 13 Hz, $^1J_{PtC}$ = 719 Hz, Pt*C*=CH). The β-vinylic carbon signal was not assigned. $^{31}P\{^1H\}$ NMR (CD_2Cl_2, 20 °C): δ 1.5 (d, $^2J_{PP}$ = 16 Hz, $^1J_{PtP}$ = 2063 Hz, $^2J_{^{119}SnP}$ = 1723 Hz, $^2J_{^{117}SnP}$ = 1677 Hz), −1.1 (d, $^2J_{PP}$ = 16 Hz, $^1J_{PtP}$ = 1965 Hz, $^2J_{^{119}SnP}$ = 166 Hz, $^2J_{^{117}SnP}$ = 160 Hz). Anal. Calcd for $C_{45}H_{52}P_2SiSnPt$: C, 54.23; H, 5.26. Found: C, 53.98; H, 5.30.

Complex 3h. ^1H NMR (CD_2Cl_2, 20 °C): δ −0.12 (s, $^3J_{PtH}$ = 7.2 Hz, $^2J_{SnH}$ = 37.2 Hz, 9H, SnMe), 0.49 (s, 3H, SiMe), 0.69 (s, 3H, SiMe), 1.07 (d, $^2J_{PH}$ = 8.4 Hz, $^3J_{PtH}$ = 25.8 Hz, 3H, PMe), 1.14 (d, $^2J_{PH}$ = 8.1 Hz, $^3J_{PtH}$ = 23.4 Hz, 3H, PMe), 1.47 (d, $^2J_{PH}$ = 7.8 Hz, $^3J_{PtH}$ = 22.8 Hz, 3H, PMe), 1.57 (d, $^2J_{PH}$ = 8.1 Hz, $^3J_{PtH}$ = 24.9 Hz, 3H, PMe), 3.64 (s, 2H, NH_2), 6.6−7.7 (m, 20H, PtC=C*H* and Ph). $^{13}C\{^1H\}$ NMR (CD_2Cl_2, 20 °C): δ −4.2 (dd, $^3J_{PC}$ = 10 and 2 Hz, $^2J_{PtC}$ = 78 Hz, $^1J_{SnC}$ = 189 Hz, SnMe), 0.39 (s, SiMe), 13.2 (dd, $^1J_{PC}$ = 26 Hz, $^3J_{PC}$ = 2 Hz, $^2J_{PtC}$ = 28 Hz, PMe), 14.5 (dd, $^1J_{PC}$ = 30 Hz, $^3J_{PC}$ = 3 Hz, $^2J_{PtC}$ = 40 Hz, PMe), 18.7 (dd, $^1J_{PC}$ = 5 Hz, $^3J_{PC}$ = 3 Hz, $^2J_{PtC}$ = 31 Hz, PMe), 19.1 (t, $^1J_{PC}$ = 9 Hz, $^2J_{PtC}$ = 39 Hz, PMe), 114.2 (s, Ar), 123.8 (t, $^3J_{PC}$ = 6 Hz, $^2J_{PtC}$ = 57 Hz, PtC=*C*H), 127.8 (s, SiPh), 128.4 (s, SiPh), 128.4 (d, $^3J_{PC}$ = 9 Hz, PPh), 128.5 (d, $^3J_{PC}$ = 9 Hz, PPh), 129.6 (d, $^4J_{PC}$ = 2 Hz, PPh), 129.7 (d, $^4J_{PC}$ = 2 Hz, PPh), 130.3 (d, $^4J_{PC}$ = 2 Hz, $^3J_{PtC}$ = 48 Hz, Ar), 130.7 (d, $^2J_{PC}$ = 12 Hz, $^3J_{PtC}$ = 14 Hz, PPh), 130.9 (d, $^2J_{PC}$ = 12 Hz, $^3J_{PtC}$ = 15 Hz, PPh), 134.3 (s, SiPh), 138.3 (dd, $^1J_{PC}$ = 36 Hz, $^3J_{PC}$ = 2 Hz, $^2J_{PtC}$ = 17 Hz, PPh), 139.1 (dd, $^1J_{PC}$ = 42 Hz, $^3J_{PC}$ = 4 Hz, $^2J_{PtC}$ = 15 Hz, PPh), 143.3 (s, SiPh), 144.0 (dd, $^3J_{PC}$ = 6 and 2 Hz, $^2J_{PtC}$ = 38 Hz, Ar), 145.5 (s, $^5J_{PtC}$ = 6 Hz, Ar), 178.2 (dd, $^2J_{PC}$ = 99 and 13 Hz, $^1J_{PtC}$ = 699 Hz, Pt*C*=CH). $^{31}P\{^1H\}$ NMR (CD_2Cl_2, 20 °C): δ −13.5 (d, $^2J_{PP}$ = 18 Hz, $^1J_{PtP}$ = 2091 Hz, $^2J_{^{119}SnP}$ = 1782 Hz, $^2J_{^{117}SnP}$ = 1703 Hz), −16.3 (d, $^2J_{PP}$ = 17 Hz, $^1J_{PtP}$ = 1891 Hz, $^2J_{^{119}SnP}$ = 168 Hz, $^2J_{^{117}SnP}$ = 160 Hz). Anal. Calcd for $C_{35}H_{49}NP_2SiSnPt$: C, 47.36; H, 5.56; N, 1.58. Found: C, 47.33; H, 5.51; N, 1.62.

Complex 3i. ^1H NMR (CD_2Cl_2, 20 °C): δ −0.11 (s, $^3J_{PtH}$ = 7.5 Hz, $^2J_{SnH}$ = 37.5 Hz, 9H, SnMe), 0.50 (s, 3H, SiMe), 0.70 (s, 3H, SiMe), 1.04 (d, $^2J_{PH}$ = 8.7 Hz, $^3J_{PtH}$ = 25.2 Hz, 3H, PMe), 1.14 (d, $^2J_{PH}$ = 8.4 Hz, $^3J_{PtH}$ = 22.8 Hz, 3H, PMe), 1.48 (d, $^2J_{PH}$ = 7.8 Hz, $^3J_{PtH}$ = 22.8 Hz, 3H, PMe), 1.58 (d, $^2J_{PH}$ = 8.1 Hz, $^3J_{PtH}$ = 25.2 Hz, 3H, PMe), 2.33 (s, 3H, Me), 7.0−7.7 (m, 20H, PtC=C*H* and Ph). $^{13}C\{^1H\}$ NMR (CD_2Cl_2, 20 °C): δ −4.2 (dd, $^3J_{PC}$ = 10 and 1 Hz, $^2J_{PtC}$ = 79 Hz, $^1J_{SnC}$ = 190 Hz, SnMe), 0.24 (s, SiMe), 13.3 (dd, $^1J_{PC}$ = 26 Hz, $^3J_{PC}$ = 2 Hz, $^2J_{PtC}$ = 26 Hz, PMe), 14.5 (dd, $^1J_{PC}$ = 30 Hz, $^3J_{PC}$ = 3 Hz, $^2J_{PtC}$ = 39 Hz, PMe), 18.7 (dd, $^1J_{PC}$ = 15 Hz, $^3J_{PC}$ = 6 Hz, $^2J_{PtC}$ = 20 Hz, PMe), 19.2 (dd, $^1J_{PC}$ = 16 Hz, $^3J_{PC}$ = 4 Hz, $^2J_{PtC}$ = 40 Hz, PMe), 21.1 (s, Me), 127.0 (t, $^3J_{PC}$ = 7 Hz, $^2J_{PtC}$ = 57 Hz, PtC=*C*H), 127.8 (s, SiPh), 128.4 (s, SiPh), 128.4 (d, $^3J_{PC}$ = 9 Hz, PPh), 128.4 (s, Ar), 128.5 (d, $^3J_{PC}$ = 9 Hz, PPh), 129.2 (d, $^4J_{PC}$ = 2 Hz, $^3J_{PtC}$ = 51 Hz, Ar), 129.6 (d, $^4J_{PC}$ = 2 Hz, PPh), 129.7 (d, $^4J_{PC}$ = 2 Hz, PPh), 130.8 (d, $^2J_{PC}$ = 12 Hz, $^3J_{PtC}$ = 14 Hz, PPh), 130.9 (d, $^2J_{PC}$ = 11 Hz, $^3J_{PtC}$ = 16 Hz, PPh), 134.3 (s, SiPh), 135.8 (s, $^5J_{PtC}$ = 6 Hz, Ar), 138.1 (dd, $^1J_{PC}$ = 36 Hz, $^3J_{PC}$ = 2 Hz, $^2J_{PtC}$ = 16 Hz, PPh), 138.9 (dd, $^1J_{PC}$ = 42 Hz, $^3J_{PC}$ = 4 Hz, $^2J_{PtC}$ = 14 Hz, PPh), 143.0 (s, SiPh), 150.6 (dd, $^3J_{PC}$ = 6 and 2 Hz, $^2J_{PtC}$ = 38 Hz, Ar), 178.9 (dd, $^2J_{PC}$ = 100 and 13 Hz, $^1J_{PtC}$ = 705 Hz, Pt*C*=CH). $^{31}P\{^1H\}$ NMR (CD_2Cl_2, 20 °C): δ −13.9 (d, $^2J_{PP}$ = 17 Hz, $^1J_{PtP}$ = 2079 Hz, $^2J_{^{119}SnP}$ = 1776 Hz, $^2J_{^{117}SnP}$ = 1696 Hz), −16.6 (d, $^2J_{PP}$ = 17 Hz, $^1J_{PtP}$ = 1919 Hz, $^2J_{^{119}SnP}$ = 168 Hz, $^2J_{^{117}SnP}$ = 160 Hz). Anal. Calcd for $C_{36}H_{50}P_2SiSnPt$: C, 48.77; H, 5.68. Found: C, 48.42; H, 5.71.

Complex 3j. ^1H NMR (CD_2Cl_2, 20 °C): δ −0.12 (s, $^3J_{PtH}$ = 7.2 Hz, $^2J_{SnH}$ = 35.7 Hz, 9H, SnMe), 0.51 (s, 3H, SiMe), 0.71 (s, 3H, SiMe), 1.04 (d, $^2J_{PH}$ = 8.7 Hz, $^3J_{PtH}$ = 24.6 Hz, 3H, PMe), 1.14 (d, $^2J_{PH}$ = 8.1 Hz, $^3J_{PtH}$ = 23.4 Hz, 3H, PMe), 1.50 (d, $^2J_{PH}$ = 8.1 Hz, $^3J_{PtH}$ = 23.4 Hz, 3H, PMe), 1.59 (d, $^2J_{PH}$ = 8.1 Hz, $^3J_{PtH}$ = 27.6 Hz, 3H, PMe), 7.0−7.9 (m, 20H, PtC=C*H* and Ph), 9.95 (s, 1H, CHO). $^{13}C\{^1H\}$ NMR (CD_2Cl_2, 20 °C): δ −4.2 (dd, $^3J_{PC}$ = 10 and 2 Hz, $^2J_{PtC}$ = 76 Hz, $^1J_{SnC}$ = 196 Hz, SnMe), 0.0 (s, SiMe), 13.4 (dd, $^1J_{PC}$ = 26 Hz, $^3J_{PC}$ = 2 Hz, $^2J_{PtC}$ = 27 Hz, PMe), 14.7 (dd, $^1J_{PC}$ = 30 Hz, $^3J_{PC}$ = 3 Hz, $^2J_{PtC}$ = 38 Hz, PMe), 18.7 (dd, $^1J_{PC}$ = 9 Hz, $^3J_{PC}$ = 5 Hz, PMe), 19.1 (dd, $^1J_{PC}$ = 10 Hz, $^3J_{PC}$ = 5 Hz, PMe), 127.9 (s, SiPh), 128.5 (d, $^3J_{PC}$ = 9 Hz, PPh), 128.6 (m, $^3J_{PC}$ = 9 Hz, PPh), 128.7 (s, SiPh), 129.3 (s, Ar), 129.7 (d, $^4J_{PC}$ = 2 Hz, $^3J_{PtC}$ = 46 Hz, Ar), 129.7 (d, $^4J_{PC}$ = 2 Hz, PPh), 129.9 (d, $^4J_{PC}$ = 2 Hz, PPh), 130.7 (d, $^2J_{PC}$ = 12 Hz, $^3J_{PtC}$ = 14 Hz, PPh), 130.8 (d, $^2J_{PC}$ = 12 Hz, $^3J_{PtC}$ = 16 Hz, PPh), 133.1 (t, $^3J_{PC}$ = 6 Hz, $^2J_{PtC}$ = 52 Hz, PtC=*C*H), 134.3 (s, SiPh), 134.4 (s, $^5J_{PtC}$ = 6 Hz, Ar), 137.6 (dd, $^1J_{PC}$ = 37 Hz, $^3J_{PC}$ = 2 Hz, $^2J_{PtC}$ = 16 Hz, PPh), 138.9 (dd, $^1J_{PC}$ = 43 Hz, $^3J_{PC}$ = 3 Hz, $^2J_{PtC}$ = 14 Hz, PPh), 142.2 (s, SiPh), 159.7 (dd, $^3J_{PC}$ = 6 and 2 Hz, $^2J_{PtC}$ = 36 Hz, Ar), 177.6 (dd, $^2J_{PC}$ = 100 and 13 Hz, $^1J_{PtC}$ = 716 Hz, Pt*C*=CH), 192.3 (s, CHO). $^{31}P\{^1H\}$ NMR (CD_2Cl_2, 20 °C): δ −13.9 (d, $^2J_{PP}$ = 18 Hz, $^1J_{PtP}$ = 2041 Hz, $^2J_{^{119}SnP}$ = 1747 Hz, $^2J_{^{117}SnP}$ = 1671 Hz), −16.7 (d, $^2J_{PP}$ = 18 Hz, $^1J_{PtP}$ = 1968 Hz, $^2J_{^{119}SnP}$ = 166 Hz, $^2J_{^{117}SnP}$ = 158 Hz). Anal. Calcd for $C_{36}H_{48}P_2OSiSnPt$: C, 48.01; H, 5.37. Found: C, 48.05; H, 5.35.

Kinetic Study. Complex **1b** (11.5 mg, 14.9 μmol) and PhC≡CH (9.2−35.5 mg) were placed in an NMR sample tube equipped with a rubber septum cap and dissolved at −50 °C in CD_2Cl_2 containing free PMe_2Ph (2.5−30 mM) to obtain a total volume of the solution of 0.6 mL. The sample tube was placed in an NMR sample probe controlled at −5.0 ± 0.1 °C and examined at intervals by ^1H NMR spectroscopy. The amounts of **1b**, **2b**, and **3b** at time *t* were determined by peak integration of the $SnMe_3$ signals at δ −0.02 (**1b**), 0.24 (**2b**), and −0.17 (**3b**).

Crossover Experiments for the Conversion of 2b to 3b. Complex **1b** (11.5 mg, 14.9 μmol) was dissolved in CD_2Cl_2 (0.6 mL) containing free PMe_2Ph (2.5 mM) at −50 °C. Phenylacetylene (1.6 μL, 14.6 μmol) was added, and the sample solution was allowed to stand at −5 °C for 1 h. The $^{31}P\{^1H\}$ NMR analysis revealed the formation of **2b** and **3b** in a 30/70 ratio. Then, *p*-MeC_6H_4C≡CH (5.6 μL, 44.8 μmol) was added,

Table 5. Crystal Data and Details of the Structure Determination for 1d and 2k

	1d	2k
formula	$C_{41}H_{54}OP_2SiSnPt$	$C_{33}H_{48}O_4P_2SiSnPt$
fw	966.69	912.55
cryst size, mm	0.23 × 0.2 × 0.2	0.2 × 0.2 × 0.2
cryst syst	orthorhombic	triclinic
no. of reflns used for unit cell determination (2θ range, deg)	60511 (4.6−55.0)	25 (29.9−30.0)
a (Å)	17.8553(4)	11.845(3)
b (Å)	19.7769(6)	16.684(5)
c (Å)	11.8019(3)	10.484(3)
α (deg)		100.03(3)
β (deg)		111.73(2)
γ (deg)		75.72(2)
V (Å^3)	4167.5(2)	1857(1)
space group	$P2_12_12_1$ (#19)	$P\bar{1}$ (#2)
Z	4	2
d_{calcd} (g cm^{-3})	1.541	1.632
μ(Mo Kα) (cm^{-1})	40.73	45.70
diffractometer	Rigaku RAXIS-RAPID (imaging plate)	Rigaku AFC7R (ω−2θ scan)
temp, °C	22	−75
2θ max (deg)	55.0	55.0
no. of reflns collected	38954	9066
no. of unique reflns	5282 (R_{int} = 0.078)	3025 (R_{int} = 0.025)
transmn factors	0.3277−0.5056	0.3635−0.9991
no. of obsd reflns	4562 ($I \geq 3.0\sigma(I)$)	8381 ($I \geq 3.0\sigma(I)$)
no. of variables	401	380
R indices ($I \geq 3\sigma(I)$)[a]	R_1 = 0.028 R = 0.046 R_w = 0.061 GOF = 1.01	R_1 = 0.052 R = 0.088 R_w = 0.197 GOF = 1.55
max. Δ/σ in final cycle	0.000	0.003
max. and min. peak (e Å^{-3})	0.63, −1.21	1.98, −4.11

[a] Function minimized = $\sum w(F_o^2 - F_c^2)^2$; $w = (1/[\sigma^2(F_o^2)])$. $R_1 = \sum||F_o| - |F_c||/\sum|F_o|$. $R = \sum(F_o^2 - F_c^2)/\sum(F_o^2)$. $R_w = [\sum w(F_o^2 - F_c^2)^2/\sum w(F_o^2)^2]^{1/2}$. GOF = $[\sum w(|F_o| - |F_c|)^2/(N_o - N_v)]^{1/2}$, where N_o and N_v stand for the number of observations and variables, respectively.

and the sample was warmed at 35 °C for 3 h. The $^{31}P\{^1H\}$ NMR spectrum measured at 20 °C showed complete conversion of **2b** to **3b**. In the ^1H NMR spectrum, no trace of the methyl proton signal of **3i** at δ 2.33 was detected, while the signal due to the methyl group of *p*-$MeC_6H_4C{\equiv}CH$ at δ 2.48 remained unchanged. A similar experiment was carried out using PhC≡CH (3 equiv) and a 28/78 mixture of **2i** and **3i**. In this case, no trace of the methyl proton signal of free *p*-$MeC_6H_4C{\equiv}CH$ at δ 2.48 was detected.

X-ray Structural Analysis. (a) Data Collection. 1d·THF: A yellow block crystal having approximate dimensions of 0.23 × 0.2 × 0.2 mm, which was grown from a mixed solvent of THF and Et_2O at −25 °C, was mounted on a glass fiber. All measurements were made on a Rigaku RAXIS-RAPID imaging plate diffractometer with graphite-monochromated Mo Kα radiation (λ = 0.71069 Å). Indexing was performed from 1 oscillation which was exposed for 2.5 min. Based on the unit cell dimensions and systematic absences in the diffractometer data ($h00$: $h \neq 2n$; $0k0$: $k \neq 2n$; $00l$: $l \neq 2n$), the space group was uniquely determined to be $P2_12_12_1$ (#19). The data were collected at 22 ± 1 °C to a maximum 2θ value of 55.0°. A total of 80 images, corresponding to 222.5° oscillation angles, were collected with two different goniometer settings. Exposure time was 1.70 min per degree. The camera radius was 127.40 mm. Readout was performed in the 0.150 mm pixel mode. Of the 38 954 reflections collected, 5282 were unique (R_{int} = 0.078); equivalent reflections were merged. The data were corrected for Lorentz and polarization effects and absorption (NUMABS).

Complex 2k. An orange crystal having approximate dimensions of 0.2 × 0.2 × 0.2 mm, which was grown by slow diffusion of a CH_2Cl_2 solution in pentane at −25 °C, was mounted on a glass fiber. All measurements were performed on a Rigaku AFC7R four-circle diffractometer with graphite-monochromated Mo Kα radiation (λ = 0.71069 Å). Unit cell dimensions were obtained from a least-squares treatment of the setting angles of 25 automatically centered reflections with $\theta > 25°$. The unit cell dimensions, a statistical analysis of intensity distribution, and the successful solution and refinement of the structure indicated the space group $P\bar{1}$ (#2). The intensity data were collected at −75 ± 1 °C to a maximum 2θ value of 55.0° using ω−2θ scan technique at a scan rate of 16 deg/min^{-1} in omega. Of the 9066 reflections collected, 3025 were unique (R_{int} = 0.025). The data were corrected for Lorentz and polarization effects, decay (5.4%, based on three standard reflections monitored at every 150 reflection measurements), and absorption (empirical, based on azimuthal scans of three reflections).

(b) Structure Solution and Refinement. All calculations were performed with the TEXSAN Crystal Structure Analysis Package provided by Rigaku Corp. The structure was solved by heavy atom Patterson methods (PATTY) and expanded using Fourier techniques (DIRDIF94). All non-hydrogen atoms, except for the carbon and oxygen atoms of the crystal solvent in **1d**·THF, were refined anisotropically. In the final cycles of refinement, hydrogen atoms were located at idealized positions (d(C−H) = 0.95 Å) with isotropic temperature factors ($B_{iso} = 1.20B_{bonded\ atom}$) and were included in calculation without refinement of their parameters. The function minimized in least-squares was $\sum w(F_o^2 - F_c^2)^2$ ($w = 1/[\sigma^2(F_o^2)]$). Crystal data and details of data collection and refinement are summarized in Table 5. Additional information is available as Supporting Information.

Acknowledgment. This work was supported by a Grant-in-Aid for Scientific Research from the Ministry of Education, Culture, Sports, Science and Technology, Japan.

Supporting Information Available: Details of the structure determination of **1d** and **2k**, including figures giving the atomic numbering schemes and tables of atomic coordinates, thermal parameters, and full bond distances and angles. This material is available free of charge via the Internet at http://pubs.acs.org.

OM030553T